NASA TECHNICAL NOTE

NASA TN D-8334 c.1

NASA TN D-8334

SCRAMJET NOZZLE DESIGN AND ANALYSIS AS APPLIED TO A HIGHLY INTEGRATED HYPERSONIC RESEARCH AIRPLANE

William J. Small, John P. Weidner, and P. J. Johnston

Langley Research Center
Hampton, Va. 23665

NATIONAL AERONAUTICS AND SPACE ADMINISTRATION • WASHINGTON, D. C. • NOVEMBER 1976

1. Report No.	2. Government Accession No.	
NASA TN D-8334		

4. Title and Subtitle	5. Report Date
SCRAMJET NOZZLE DESIGN AND ANALYSIS AS APPLIED TO A HIGHLY INTEGRATED HYPERSONIC RESEARCH AIRPLANE	November 1976
	6. Performing Organization Code
7. Author(s) William J. Small, John P. Weidner, and P. J. Johnston	8. Performing Organization Report No. L-11003
	10. Work Unit No. 505-11-31-02
9. Performing Organization Name and Address NASA Langley Research Center Hampton, VA 23665	11. Contract or Grant No.
	13. Type of Report and Period Covered Technical Note
12. Sponsoring Agency Name and Address National Aeronautics and Space Administration Washington, DC 20546	14. Sponsoring Agency Code

15. Supplementary Notes

16. Abstract

The great potential expected from future air-breathing hypersonic aircraft systems is predicated on the assumption that the propulsion system can be efficiently integrated with the airframe. A study of engine-nozzle airframe integration at hypersonic speeds has been conducted by using a high-speed research-aircraft concept as a focus. Recently developed techniques for analysis of scramjet-nozzle exhaust flows provide a realistic analysis of complex forces resulting from the engine-nozzle airframe coupling. Results from these studies show that by properly integrating the engine-nozzle propulsive system with the airframe, efficient, controlled and stable flight results over a wide speed range.

17. Key Words (Suggested by Author(s))	18. Distribution Statement
Engine-airframe integration Hypersonic propulsion Scramjet propulsion	Unclassified - Unlimited Subject Category 02

19. Security Classif. (of this report)	20. Security Classif. (of this page)	21. No. of Pages	22. Price*
Unclassified	Unclassified	45	$3.75

* For sale by the National Technical Information Service, Springfield, Virginia 22161

SCRAMJET NOZZLE DESIGN AND ANALYSIS AS APPLIED TO A HIGHLY INTEGRATED HYPERSONIC RESEARCH AIRPLANE

William J. Small, John P. Weidner, and P. J. Johnston
Langley Research Center

SUMMARY

The great potential expected from future air-breathing hypersonic aircraft systems is predicated on the assumption that the propulsion system can be efficiently integrated with the airframe. A study of engine-nozzle airframe integration at hypersonic speeds has been conducted by using a high-speed research-aircraft concept as a focus. Recently developed techniques for analysis of scramjet-nozzle exhaust flows provide a realistic analysis of complex forces resulting from the engine-nozzle airframe coupling. Results from these studies show that by properly integrating the engine-nozzle propulsive system with the airframe, efficient, controlled and stable flight results over a wide speed range.

INTRODUCTION

Studies of hypersonic air-breathing aircraft using hydrogen fuel have shown them to have unique and desirable characteristics as future flight systems (refs. 1 to 5). The high speeds typical of these vehicles make them attractive for a variety of missions such as long-range civil transports, launch vehicles for second-stage orbiters, and a variety of military applications. The expected flight regimes of these aircraft are illustrated in figure 1. Efficient air-breathing propulsion systems utilizing ramjet-scramjet engine cycles are critical developmental items and constitute a pacing item in hypersonic aircraft development. The propulsion-system installation for very high-speed flight will differ from conventional concepts in that a higher degree of commonality is required between airframe and engine components.

As illustrated in figure 2, the entire vehicle undersurface is devoted to the propulsion system. The forebody acts as an inlet compression ramp, a center portion of the body contains engine modules, and the complete afterbody forms an exhaust-nozzle surface.

Previous studies (refs. 6 to 8) have found these integrated concepts to have beneficial aspects for both cruise and acceleration applications. Advantages that accrue from efficient engine-airframe integration include forebody inlet precompression, which effectively reduces required engine size and weight requirements as compared to a free-stream inlet; and because some of the work of inlet compression has been accomplished by this forebody, overall engine efficiency is improved. Exhaust-nozzle performance also benefits from this integrated concept because the large afterbody nozzle area can potentially provide very efficient exhaust-gas expansion with minimal aerodynamic drag. This large

exhaust surface can also be used advantageously to increase favorable lift for cruise aircraft.

Integration of engine and airframe in this highly integrated manner, however, is not the only solution to the design of hypersonic propulsion systems. An alternate concept incorporates axisymmetric engines and nozzles contained within discrete nacelles in a manner similar to current podded turbojet engines. The study of reference 9 specifically addresses these alternate concepts and concludes that integrated systems such as those studied in this paper offer a much higher installed specific impulse as compared to axisymmetric systems.

It is apparent that the large exhaust surfaces of highly coupled, integrated aircraft can produce large thrust and moment forces, and in the case of an improperly designed nozzle, associated trim drag penalties may become excessive. Because nozzle design is primarily controlled by thrust and stability requirements, it is imperative that propulsion-system parameters be examined across the entire aircraft flight envelope. Vehicle trim capability in the power-off mode also assumes increased importance owing to the possible large shift in thrust vectors and resulting trim requirements. Therefore, one key to a successful high-performance vehicle is a systematic procedure for effectively assessing these interactions in the early stages of a design if any beneficial coupling between the engine, nozzle, and airframe is to be achieved.

A study of the interactions between propulsion and aerodynamics of a highly integrated vehicle was undertaken in support of a Langley Research Center research airplane conceptual design effort and is partly described in references 10 and 11. Its mission was to act as a test vehicle for key hypersonic technology items such as structural and thermal protection-system concepts, and propulsion package operation under true flight conditions throughout most of the hypersonic flight regime of interest (fig. 1). Propulsion-system concepts and trends developed during the course of this study, because of the highly integrated nature of this vehicle and the large range of flight conditions that had to be evaluated, should apply to a large class of hypersonic vehicles. The results, concepts, and techniques developed for engine-nozzle-airframe integration as a result of this study form the subject of this paper.

The organization of the paper is summarized as follows:

(1) General study considerations: Background material is presented for the research vehicle and scramjet-engine module of this study. Fundamental engine sizing constraints are also discussed.

(2) Analytical techniques: Ground rules for this study and analytical methods for computing airframe and propulsion-system components are summarized. Engine-airframe force-data bookkeeping procedures are outlined.

(3) Parametric study of nozzle: Nozzle geometry and longitudinal engine-nozzle locations are parametrically varied to determine their effect on nozzle operation and the resulting integrated trimmed vehicle performance.

(4) Propulsion effects on vehicle performance: A candidate nozzle determined to be near optimum from the previous parametric study is used to investigate vehicle stability and acceleration performance.

SYMBOLS

A	area
A_i	inlet area
A_1	inlet capture area
A_4	ideal one-dimensional exhaust area
C_L	lift coefficient, $\frac{\text{Lift}}{q_\infty S_{ref}}$
C_m	pitching-moment coefficient, $\left(\frac{\text{Pitching moment}}{\text{Vehicle length}}\right) \Big/ q_\infty S_{ref}$
C_S	spillage force coefficient
C_T	thrust coefficient in flight direction, $\frac{T}{q_\infty S_{ref}}$
C_{T_e}	engine thrust coefficient in plane of engine, $\frac{\text{Engine thrust}}{q_\infty S_{ref}}$
C_{T_s}	cowl thrust coefficient, $\frac{\text{Cowl force}}{q_\infty S_{ref}}$
C_{T_w}	nozzle-wall thrust coefficient, $\frac{\text{Wall force}}{q_\infty S_{ref}}$
C_σ	isolated-nozzle thrust coefficient
D	drag
F_x	axial-inlet spillage force
F_y	normal-inlet spillage force
H_2	hydrogen
h_c	combustor exit height
h_i	inlet height

I_{sp}	specific impulse
L/D	lift-drag ratio
l	length
M	Mach number
p	pressure
q	dynamic pressure, Pa (lbf/ft^2)
S_{ref}	vehicle reference area
T	thrust; temperature, K
V	velocity, m/sec
V_s	satellite velocity
x_{ac}	aerodynamic-center location
α	angle of attack; incidence, deg
δ_e	elevon deflection angle, positive when trailing edge is down, deg
θ	surface incidence, deg
σ	angle between engine-nozzle axis and flight direction
ϕ	equivalence ratio, percent of stoichiometric fuel-to-air ratio

Subscripts:

c	combustor exit
e	engine
i	inlet
m	moment
n	nozzle
s	cowl
v	vehicle
w	wall
x	axial direction

y	normal direction
1	airflow properties prior to inlet entrance
3	combustor-exit conditions
∞	free stream

GENERAL STUDY CONSIDERATIONS

A Langley Research Center design study of conceptual high-speed research airplanes investigated a series of alternate candidate concepts. From these concepts a highly integrated hydrogen-fueled design was selected as the focus for this propulsion integration study because it incorporated many of the significant features of future hypersonic aircraft, such as large afterbody areas for nozzle expansion. This vehicle and its associated scramjet propulsion package are next summarily described.

Hydrogen-Fueled Hypersonic Research Aircraft

The hypersonic research aircraft used as the basis for the engine-nozzle-vehicle integration analysis described in this paper (figs. 2 and 3), is 24.38 meters long and is powered by four rocket engines fueled with liquid hydrogen and liquid oxygen. Sufficient propellant is contained within the aircraft for rocket acceleration to Mach 8 from an air launch at Mach 0.8, with additional propellant for Mach 10 boost provided by external tanks that would jettison at about Mach 2. As illustrated in figures 2 and 3, six research scramjet modules can be integrated with the basic aircraft. With efficient integration the scramjets can provide accelerating thrust between Mach 4 and 10 without rocket power.

LRC Fixed-Geometry Scramjet

The baseline research scramjet employed in this study is the fixed-geometry concept currently under development at Langley Research Center (refs. 9, 10, 12, and 13). This is a rectangular modular engine that attaches directly to the vehicle undersurface. This concept uses swept compression surfaces and fuel-injector struts to provide inlet starting at low speed and good internal performance throughout the scramjet operating speed range. The swept compression surfaces also provide localized pressure relief along the top surface of the engine to enable the scramjet to ingest the vehicle forebody boundary layer, thus eliminating the need for boundary-layer diversion or bleed. Instream fuel injection is used to minimize the combustor length and heat flux to the internal surfaces. The engine operates in a supersonic combustion mode at speeds above Mach 5. Calculations show thermal choking within the combustor may occur below Mach 5 if supersonic combustion were attempted and may result in a mode of operation involving both subsonic and supersonic combustion.

Engine Size Constraints

A primary objective of the conceptual research aircraft study was to define an integrated vehicle air-breathing propulsion system capable of demonstrating acceleration and high-component performance throughout a wide hypersonic speed range. Mission analysis studies indicated that good aircraft acceleration throughout the scramjet operating range was of paramount importance. Accordingly, the engine inlet was always sized to take full advantage of the maximum usable area within the forebody shock layer. Inlets designed to extend through the shock layer into free-stream flow are considered unlikely possibilities from the standpoint of reduced engine performance and increased weight requirements and were not considered. Increased Mach number generally requires an increasing engine size as a result of reduced air density and specific impulse. At the same time increased Mach number decreases the depth of the forebody lower surface shock layer such that the inlet must be located at a more rearward body station where sufficient airflow is available. The vehicle forebody has a major influence on the size engine that can be installed at any given body station through minimizing flow angularity and maximizing available mass flow available for processing at the inlet face. A good forebody design allows a maximum utilization of the available area within the body shock layer. Details of the forebody design and analysis are discussed in reference 10.

While the effect of higher Mach numbers is to move the engine location rearward to maximize engine size, at the same time the larger nozzle expansion areas needed to maximize thrust at higher Mach numbers have the effect of increasing nozzle length and forcing the engine forward. Figure 4 illustrates the ideal expansion area required for fully expanded nozzles for the case of isentropically expanding hydrogen-air combustion products. The isentropic conditions shown represent uniform parallel entrance and exit nozzle flows expanding to a single specified exit pressure. Practically, however, such a nozzle is too long for most hypersonic aircraft applications, and true nozzle exit conditions are far from uniform. This nonuniformity results from the fact that the nozzle upper wall has the capability to expand to near-stream pressure before overexpanding, yet the nozzle interior cowl wall pressure can only expand to the higher external cowl pressure before it overexpands. Nonetheless, the manner in which ideal exhaust-expansion-area requirements tend to increase with Mach number is, in general, indicative of the trend of practical nozzles.

ANALYTICAL TECHNIQUES

A complete analysis of the impact of propulsion-system variables on total aircraft performance involves a large spectrum of flight conditions for each propulsion-system variable considered. The preliminary analysis reported herein, however, confined the engine-nozzle-airframe design study to a 71 820-Pa (1500-lbf/ft^2) acceleration flight path from Mach 4 (scramjet ignition) to Mach 10 (maximum aircraft Mach number). The engine-nozzle-airframe combination was analyzed at an aircraft angle of attack of 2°, which was representative of the 71 820-Pa flight path, and total-trimmed-aircraft thrust margin was the primary criterion for evaluating the engine-nozzle combinations. The propulsion system was analyzed at the discrete Mach numbers of 4, 6, and 10, and the

following Mach number—fuel-air ratio schedule was determined to be near optimum from missions studied:

M_∞	ϕ
4	1.0
6	1.0
10	1.5

Several analytical methods were required to compute the major airframe, engine, and nozzle forces, and the essential elements of these techniques are now summarized.

Airframe Analysis

Aerodynamics of the basic vehicle and external engine cowl surfaces were evaluated using the hypersonic arbitrary-body program of reference 14 by selecting the following program options. Body and cowl compression surface pressures were computed using tangent-cone methods, and compression surface pressures on wings, tails, and control surfaces were computed using tangent-wedge methods. All pressure on aerodynamic surfaces in expansion was determined by Prandtl-Meyer expansion from free stream. Turbulent skin friction was calculated by the method of Spalding and Chi.

Engine Analysis

Engine-module performance was analyzed by using one-dimensional techniques for either a pure scramjet cycle (refs. 9 and 13) or pure ramjet cycle (ref. 15). Scramjet (supersonic combustion) engine performance was calculated at discrete Mach numbers of 4, 6, and 10, and ramjet (subsonic combustion) engine-module performance was calculated at Mach 4. Mission analysis studies for this vehicle indicated that fuel-to-air ratios near stoichiometric were required to produce acceptable acceleration performance at Mach 4. A fuel-to-air ratio near stoichiometric could not be obtained in a pure scramjet cycle at this low Mach number because of thermal choking. Therefore, for the purposes of this study, ramjet engine performance was used at Mach 4 and scramjet engine performance was used at Mach 6 and 10. These calculations were used not only to assess internal engine performance but also to provide the initial conditions for the nozzle calculations. Inlet-entrance and combustor-exit conditions are presented in table 1.

Nozzle Analysis

Six discrete scramjet modules were combined to form the complete engine system for the aircraft as shown in figures 2 and 3. Uniform two-dimensional flow exhausting from a single combustor exit was assumed to represent the engine package; thus, for purposes of this study the assumption was made that combustor-

exit geometry, instead of forming a series of six discrete rectangular combustor exits exhibiting three-dimensional flow, would be modified to a single rectangular two-dimensional exit spanning the entire width of the engine package. In order to preserve exit area with this greater width, the two-dimensional combustor-exit height was reduced from the three-dimensional case. In all cases presented in this paper, the resulting two-dimensional ratio of combustor-exit height to engine-inlet height is held constant.

Nozzle forces were analyzed by using a recently developed three-dimensional reference-plane characteristics computer program in a two-dimensional mode of operation (refs. 16 and 17). As stated previously, engine-cycle calculations were used to obtain initial conditions, and thereafter exhaust-gas properties were internally generated by the nozzle program for proper hydrogen-air combustion product mixtures in local chemical equilibrium. The interaction between nozzle flow and external flow was computed for all cases of nozzle underexpansion. Nozzle geometry was assumed strictly two-dimensional from the combustor-exit plane rearward (fig. 5). Nozzle-wall contours were linear segments joined by small radii to insure surface slope continuity. Note that combustor-exit conditions are assumed to begin in a vertical rather than the sweptback plane typical of this engine concept. It is realized that three-dimensional effects are of importance in nozzle design; however, in this preliminary effort emphasis was placed on major trends in nozzle design that could be discerned without the additional complexity of three dimensionality. Subsequent analysis should investigate three-dimensional effects to the limit of available theoretical and experimental methods.

External Cowl Surfaces

Sidewall surfaces of the engine cowling were approximately alined with the flow under the body. The cowling lower surface, on the other hand, is inclined into the flow with an angle determined by the nozzle-cowl-wall geometry (fig. 5). Changes in this nozzle-cowl-wall geometry thus necessarily involve changes in exterior-cowl aerodynamic forces, which were accounted for in all integrated vehicle calculations. As a result of the forebody analysis of reference 10, the engine-inlet cowling was designed to subtend approximately 80 percent of the body lower surface width as shown in figure 3. For this vehicle, this is the maximum engine width commensurate with reasonably uniform flow within the forebody shock-layer flow.

Engine Spillage

Engine spillage is a design feature of this fixed-geometry engine that allows operation at low Mach numbers. The spillage schedule was taken from reference 13 (fig. 6(a)) and was used in computing engine performance. Spillage forces are caused by the deflection of spillage air by the engine-inlet external shock system and are presented in figure 6(b). These values were computed through a theoretical evaluation of integrated forces along the engine-spillage stream tube. It was assumed that engine spillage did not affect engine-cowl pressures.

Definition of Forces

For purposes of analysis and presentation of data, the propulsion-system forces were subdivided into several categories, which were separately calculated and then used in the total-vehicle force integrations. One of these categories, the engine-module forces, contains all interior forces of the propulsion system from the beginning of the module inlet through the combustor. The component of engine thrust in the flight direction is denoted as net engine-module thrust. Note that the engine module develops net lift and pitching moments, which are accounted for in total-integrated vehicle-force summations.

The second general category of propulsion-system forces, the nozzle forces, includes all surface forces (upper nozzle wall and interior cowl wall) extending rearward from the combustor exit. Nozzle-force summations do not include net engine-module forces nor external cowl forces. Nozzle thrust coefficients presented in this paper are calculated in the flight-axis direction unless otherwise noted, and the nozzle moments are taken about the vehicle center of gravity (64.5 percent of body length). This center-of-gravity location is held constant throughout the study for all nozzle and engine locations. Nozzle lengths are nondimensionalized by combustor-exit height because this length-to-height ratio characterizes those parts of the nozzle geometry affected by expansion fans emanating from either the nozzle wall or cowl surfaces. Nozzle forces and moments used in this study are presented in table 2.

The last category of propulsion-system forces, external forces, includes spillage and external cowl aerodynamic forces, which are accounted for in all force summations.

Aerodynamic forces are computed over the entire vehicle surface not subtended by the propulsion-system components (inlet, exterior cowling, and nozzle). Note that the forces on the vehicle forebody ahead of the inlet entrance are not included as part of the propulsion system but rather as an integral part of the airframe aerodynamics.

PARAMETRIC STUDY OF NOZZLE

The purpose of the nozzle optimization analysis was to assess the effects of nozzle-geometry modifications (fig. 5) on aircraft performance (primarily thrust margin and trim control) and to determine optimum combinations of the nozzle variables for the research airplane configuration. The longitudinal location of the scramjet, upper nozzle-wall angle, interior cowl angle, and cowl length measured from the combustor exit were the primary independent nozzle variables used to optimize the engine-nozzle combination and its effect on vehicle performance. Note that the lower cowl exterior-surface angle was determined by the interior cowl angle θ_s and cowl length l_s.

In principle, global optimums for these variables could be found by using a parameter minimization technique. Such a procedure was impractical for this study because of the mass of data processing required to establish a single variation from a given reference point. Instead, variations in nozzle geometry were made from a baseline nozzle selected early in the study on the basis of good

performance characteristics at Mach 10, as described subsequently in the section entitled "Scramjet Location." The use of this baseline nozzle offers a convenient reference to gage the relative merits of the parametric-nozzle variations presented. The baseline-nozzle upper wall was characterized by an upper wall expansion angle of 20° and a length 18.54 times the combustor height. The nozzle lower cowl opened at an expansion angle of 6° and was 3.12 times as long as the combustor-exit height. The geometric proportions of this nozzle are depicted in the sketch of figure 5.

Scramjet Location

Early in the study, scramjet-engine longitudinal location on the aircraft at Mach 10 was found to be one of the most crucial variables to be determined. At this high-speed end of the flight trajectory, engine thrust margins decline owing to reduced engine performance. Also, vehicle-control requirements can be very severe owing to reduced static margins at these high Mach numbers. Any large control deflections at Mach 10 imply large elevon drag and heating loads.

The method used in sizing the propulsion-system package as axial location changed (fig. 7) was to increase engine-inlet area as the engine was moved rearward so as to capture the maximum available shock-layer flow. This sizing was accomplished by assuming a constant engine width of approximately 80 percent of body span and a linear variation in shock height with longitudinal position. These assumptions were shown to be reasonable from the forebody design study of reference 10. The nozzle was held to a maximum geometric expansion area by always terminating the nozzle upper wall just below the aft-mounted rocket engine (fig. 3). Under these constraints the axial location of the engine determines the nozzle upper wall expansion angle.

The optimum longitudinal engine-module-nozzle position depends on inlet mass-flow rates, nozzle efficiency, and trim drag penalties induced by the propulsion system. Rearward propulsion-system location will increase inlet area (and, consequently, mass-flow rates through the engine modules) and will directly increase engine-module thrust. Nozzle thrust, on the other hand, is not a simple function of mass-flow rates because, as the engine is moved longitudinally, nozzle geometry and, consequently, efficiency vary. Trim drag penalties can be induced by both engine location and nozzle configuration. Nozzle efficiency, or the ability to convert nozzle-entrance momentum into useful thrust, is primarily a complex function of nozzle geometry. In order to clarify the influence of this nozzle geometry on thrust efficiency, isolated nozzles with constant nozzle-entrance conditions typical of a scramjet engine operating with 8° of forebody precompression are first examined. Cowl lengths and the nozzle exit-to-entrance area ratio are also held constant. Thus, the only variables are upper wall expansion angle and length. The geometrical variations in these isolated nozzles are seen from the upper part of figure 8 to be quite similar to the variations encountered in positioning a nozzle in various longitudinal locations as shown in figure 9, but unlike the true flight case these isolated nozzles are free from variations in mass flow and nozzle exit-to-inlet area variations.

Typically, axisymmetric rocket or turbojet engine nozzles have a clearly defined nozzle exit, and the thrust vector lies in the plane of the nozzle axis. The highly integrated scramjet nozzle, on the other hand, as shown in the force diagram of figure 8, may have very large asymmetric components normal to the conventional nozzle axis (defined as parallel to the nozzle-entrance flow). Note that as a result of wall radii and angularity, nozzle-force vectors do not lie normal to their associated wall inclination angles. If nozzle efficiency is evaluated on the basis of thrust generated along the nozzle axis, the smallest expansion angle (longest nozzle) develops the largest thrust. This is to be expected (assuming inviscid flow) because small upper wall angles reduce the strength of the upper wall expansion fan and thus increase nozzle upper wall pressures. However, the thrust in the flight direction determines vehicle acceleration characteristics, and the flight axis of the research aircraft used in this study is inclined 8° to the nozzle axis. Because nozzle-thrust levels in the flight direction depend upon both the magnitude and orientation of the forces generated on the nozzle upper wall, the optimum nozzle for producing thrust in the flight direction is not the lowest expansion-angle (longest) nozzle but is shorter and has a greater upper wall expansion angle as indicated in figure 8.

For a condition of constant mass flow and in the absence of trim drag, the 20° nozzle would be selected as an optimum from an installed thrust standpoint. The true situation in regard to longitudinally placing the engine nozzle, however, is complicated by the fact that as the engine is moved rearward from the most efficient nozzle position, the nozzle assumes a less efficient shape, inlet mass flow increases, and aircraft trim requirements change. This situation can be best explained by reference to figures 9 and 10, which schematically and graphically illustrate engine-nozzle behavior with axial location. As the nozzle is shifted rearward, net engine module and cowl forces increase in direct proportion to ingested mass flow. Upper wall forces, however, decrease as the nozzle shifts rearward and also incline more into the direction of the flight axis. The net result of engine module plus nozzle forces is seen (fig. 10) to increase in net thrust levels as the nozzle is moved rearward to the 70-percent body station with only small increases past that point. Thus, increased mass flow at the rearmost engine-nozzle axial locations was more than able to compensate for the poor efficiency of the large wall angle nozzles. Trim drag penalties on the integrated aircraft are a function of nozzle thrust and lift-induced pitching moments and can strongly influence the selection of an optimum nozzle. The magnitude of wall and cowl forces presented in figures 9 and 10 shows that for the engine module located at 0.694 of body length, nozzle moments are nearly canceled by net engine-module moments. As the engine is moved aft of this location, large positive moments are introduced as a result of the reduced nozzle upper wall and increased cowl pressures, a condition which is aggravated by an increasing moment arm to the vehicle center of gravity. In actual practice the aircraft center of gravity may move somewhat rearward with aft movement of the engine and associated changes in vehicle internal packaging and structural arrangements. Such a center-of-gravity travel may be limited, however, because it aggravates an already marginal stability problem at the highest Mach numbers. (See section entitled "Longitudinal Stability.") Refined treatment of the propulsion integration problem must of course include realistic center-of-gravity travel in the design trades.

The net effect of scramjet location on thrust margin and elevon deflections required for trim is shown in figure 11 for the research airplane. As previously shown, the decrease in nozzle efficiency with the more rearward engine locations tends to counterbalance the beneficial effects of increased mass flow such that only slight increases in untrimmed thrust margins are obtained for engine locations aft of $l_e/l_v = 0.7$. However, the large positive pitching moments associated with the rearward engine location require large positive elevon trim control. As shown, trim drag associated with these positive elevon deflections prevents the most rearward nozzle from producing a maximum integrated thrust margin, despite the larger inlet capture area associated with this location. Elevon deflections are essentially zero, and the thrust margin is a maximum at an engine position $0.05l_v$ aft of the center of gravity ($l_e/l_v = 0.7$). Here nozzle forces approximately cancel engine-module moments, and the aircraft is nearly self-trimming. At the more forward engine positions the net negative pitching moments generated by the propulsion system are canceled out by negative elevon deflections, which cause a negligible drag penalty for this angle of attack of 2°. Thrust margins, however, decrease for these longer nozzles owing to large asymmetrical nozzle forces developed along the nozzle upper wall surface. For example, as shown in figure 9, the more forward nozzles (smaller wall angles) develop the largest upper wall forces but actually produce less thrust in the flight direction than the more rearward nozzles (larger wall angles).

Mission studies have shown that the assumed angle of attack of 2° closely approximates a constant 71 820-Pa (1500-lbf/ft^2) trajectory for this aircraft; however, nozzles with large elevon trim changes can be expected to deviate somewhat from this angle of attack to maintain correct lift at a constant dynamic pressure. However, moderate changes in angle of attack would not alter the basic comparisons shown in figure 11, as is shown in a subsequent section of this paper entitled "Acceleration Performance."

Parametric cowl-length variations are reviewed in a subsequent section of this paper, but at this point a brief discussion of cowl-length effects on nozzles at various longitudinal locations seems in order. Lift forces generated on upper nozzle walls and the lower cowl are each approximately three times the nozzle thrust level, and it might be suspected that variations in cowl length would provide a powerful means of controlling trim drag penalties and thus greatly influence the thrust margins presented in figure 11. In particular, a reduction in cowl length for the most rearward nozzle ($l_e/l_v = 0.775$) should reduce trim drag and thereby increase the effectiveness of this nozzle. However, as indicated in figure 12, variations in cowl length at this rearward location have little or no effect on total-vehicle thrust margins because decreases in trim drag are counterbalanced by thrust losses because of shortening the cowl. At the more forward scramjet positions, shortening the cowl significantly reduces overall nozzle thrust levels. Increases in cowl length at forward scramjet locations beyond that of the baseline nozzle ($l_s/h_c = 3.0$) tend to result in only slight improvements in thrust margin. Thus, optimum scramjet location is nearly independent of cowl length and occurs at approximately 70 percent of the length for the research vehicle concept.

Propulsion-System Analysis for Baseline Nozzle

From the preceding discussion of engine-nozzle axial location at Mach 10, an optimum location was found at 0.694 of body length. The nozzle corresponding to this location was selected as the baseline nozzle for parametric variations that follow in this paper. At this point, however, a brief analysis of propulsion-system forces and efficiencies for this baseline nozzle is presented over the operational Mach number range.

Computed integrated vehicle forces and moments are presented in figure 13 for Mach numbers of 4 to 10. Primary propulsion-system forces and moments are predominantly due to nozzle and engine components. Nozzle thrust is seen to play an increasingly critical role as the Mach number increases, and above Mach 6 nozzle thrust exceeds net engine-module thrust. Spillage and cowl forces produce net drag but are relatively insignificant compared to nozzle and engine-module thrust; these are not again presented in force breakdowns in this paper, although they have been accounted for in all integrated vehicle force and moment calculations.

The ratio of propulsion-system specific impulse to the Mach 10 value is presented for the baseline nozzle in figure 14. This impulse includes net propulsion-system forces in the flight direction from the engine-module inlet face to the nozzle exit with all pressures involved in the thrust calculation referenced to free-stream conditions. Results shown in figure 14 are very similar to those presented in references 9 and 13 which were derived from more idealized considerations.

Nozzle Expansion Area

In this section, nozzle geometric expansion area is varied by changing nozzle upper wall angle θ_w at constant scramjet location $0.7l_v$, in contrast to a previous section entitled "Scramjet Location" where wall angle was varied and geometric expansion area remained constant. The nozzle sketch shown in figure 15(a) illustrates this geometric variation. An inspection of the nozzle-wall pressure distribution (M = 10) reveals that, as could be expected, increasing wall expansion angle decreases upper wall pressures. Cowl pressures remain constant because the cowl trailing edge terminates forward of any final expansion wave emanating from the upper wall—combustor-exit juncture. Typically, those nozzles with small upper surface expansion angles generate large negative pitching moments owing to the substantial lift forces involved across the operational Mach number range of the engine.

The largest expansion-area nozzle that could be installed in the research airplane (19.8°) developed the smallest negative moment and generally counterbalanced net engine moments (fig. 15(b)). This large expansion nozzle also consistently developed the largest thrust over the speed range. Figure 16 shows the effect of integrating these nozzles with the total vehicle. The largest nozzle opening that could be fitted to the vehicle (19.8° reference nozzle) is superior to any smaller nozzle opening angle at all Mach numbers, and undoubtably a somewhat larger opening angle would improve vehicle performance to some extent at the high Mach number end of the flight regime.

The 19.8° nozzle also produces minimum trim drag (fig. 16). This nozzle requires only a 6° elevon setting variation from Mach 4 to 10 and requires the least elevon change to transition from trimmed power-on to trimmed power-off flight conditions. The effects of a fuel shutdown (power-off conditions) are characterized by engine-module drag instead of thrust and decreased nozzle upper and lower wall pressures, which for the 19.8° nozzle nearly compensate for one another.

Nozzle Cowl Angle

A part of the analysis was devoted to an examination of the effect of interior cowl-angle variations (fig. 17). Because of the large pressures developed over the relatively short cowl, its angularity might be expected to have significant effects on vehicle thrust and trim. As cowl expansion angle is increased, lower pressures are generated over both cowl and upper wall nozzle surfaces, and as a result the nozzle thrust is somewhat degraded (fig. 17(a)). The most notable effect of cowl-angle variation is in the nozzle pitching-moment characteristics at the higher Mach numbers. As the cowl angle is initially increased, reduced pressures on the upper wall and cowl surface are essentially compensating and cancel pitching-moment variations. Further expansions of the cowl to 12°, however, lower cowl pressures without a corresponding change on upper wall surfaces and result in a net positive pitching moment (fig. 17(b)). Integration of these nozzle forces with the vehicle, however, shows that superior performance levels over most of the Mach number range are achieved with the cowl angle of 6°, which most nearly balances net engine moments (fig. 18). These favorable trim conditions are reflected in the minimal elevon deflections required for the cowl angle of 6° when compared with larger or smaller cowl angles.

Nozzle-Cowl Length Variation

The length of the baseline nozzle cowl ($l_s/h_c = 3.12$) extends to a position somewhat beyond the initial expansion wave from the upper wall corner. As shown in figure 19(a), the position at which this expansion fan strikes the cowl surface results in a sudden drop in cowl pressure approximately three throat heights ($l_s/h_c \cong 3$) downstream of the nozzle throat. The baseline nozzle cowl ($l_s/h_c \cong 3.12$) was varied by shortening the cowl such that it did not extend to the initial expansion fan and also by lengthening it to extend farther into the expansion-fan pressure field. As seen in figure 19(b), the penalty for not containing all of the high-pressure flow as a result of using a short cowl was a drastic reduction in nozzle thrust brought about by lowered cowl thrust forces and by reduced upper wall pressures induced by a premature expansion fan from the cowl trailing edge. For this case nozzle upper wall lift forces are much larger than the short cowl negative lift force, and a large negative nozzle pitching moment is induced at Mach 10. Extending the nozzle cowl, however, has a beneficial effect on net nozzle thrust throughout the Mach number range and produces a net positive nozzle pitching-moment increment compared with the reference nozzle.

It was shown in the section entitled "Scramjet Location" that increasing cowl length past the reference nozzle cowl length of 3.12 does slightly increase

nozzle-thrust and vehicle-thrust margin capability at Mach 10. The fact that the same trend extends through Mach 4 is shown in figure 20. Differences between power-on and power-off trim elevon deflections also decrease for the longer cowl length. More detailed trade-offs between cowl weight, cooling requirements, and propulsion efficiency are ultimately required to select the optimum cowl length. However, in view of the small performance gains, which result from increased cowl lengths, the final cowl length may be relatively short.

PROPULSION EFFECTS ON VEHICLE PERFORMANCE

The previous sections, which focused on parametric variations of nozzle geometry and engine location, determined that for the research vehicle of this study the baseline nozzle was near optimum under all conditions studied. This baseline nozzle is now used to assess briefly propulsion effects on vehicle stability and acceleration. Results reflect integrated totals of forebody inlet compression, spillage, engine-module and nozzle efficiency, and trimmed aircraft aerodynamics through changes in angle of attack.

Longitudinal Stability

The addition of scramjet modules for power on or power off has a mixed although small effect on vehicle stability as shown in figure 21 for trimmed accelerating flight; for example, engine-power effects on stability at Mach 10 have a destabilizing influence at low angles of attack and a stabilizing effect at higher angles. Basic airframe stability parameters (aerodynamic-center location) were computed as previously described by using simplified methods, which generally predict aerodynamic centers forward of their true position. However, the implications of this stability analysis are that, for a well-designed engine-nozzle combination, longitudinal characteristics of this type of basic airframe are not seriously affected by the addition of scramjet-engine modules, either power off or power on.

Elevon deflections required for trim at angle of attack are shown in figure 22. The maximum elevon deflection needed from power-on to power-off conditions is 8°, which should be within acceptable limits; however, the dynamic behavior of such a vehicle in an engine shutdown situation is unknown and warrants further study.

Acceleration Performance

The nozzle parametric investigations of the preceding sections of this paper have led to the conclusion that, for accelerating flight, a large expansion nozzle with moderate cowl lengths and cowl deflection angles correctly located aft of the aircraft center-of-gravity position provides superior acceleration performance at an angle of attack of 2°. Realistic acceleration trajectories will deviate somewhat from such a constant angle of attack.

The ability to resolve total-vehicle forces into orthogonal lift and drag (thrust) vectors allows an investigation of acceleration performance through an

angle-of-attack range by using as a first-order criterion the following relation derived from a simple vehicle force analysis at small flight-path angles:

$$\text{Acceleration} = \frac{K\left[(T - D)/D\right]}{\left[(L/D)\Big/\left(1 - \frac{V^2}{V_s^2}\right)\right]}$$

Thrust and drag vectors are orthogonal to the lift vector, and K is a constant of proportionality. The first component of this equation, the thrust margin (T - D)/D, is examined in some detail in figure 23, which shows angle-of-attack effects on thrust and drag components for the trimmed research vehicle at Mach 10. As angle of attack increases, nozzle and engine-module thrust increase primarily as a result of increased mass flow ingested by the engine inlet and secondarily because of the greater cycle efficiency associated with reduced inlet Mach numbers. Aircraft drag typically increases with angle of attack owing to increased vehicle wave drag. Thrust margin (T - D)/D, however, peaks near an angle of attack of 2° as a result of the interplay between increased engine and nozzle thrust at angle of attack versus increasing aerodynamic drag at these higher angles. This result is shown by the thrust margin curves at the top of figure 24. Note that at lower Mach numbers maximum thrust margins also peak at low angles of attack.

Figure 24 also presents the lift-drag ratio terms contained in the acceleration equation. These integrated lift-drag ratios are summations of aerodynamic and all propulsion forces in the lift direction and are corrected for centrifugal effects. These ratios tend to peak at higher angles of attack than the thrust margins. As shown in the lower part of figure 24, maximum acceleration occurs at low angles of attack (high dynamic pressures) where minimum-drag coefficients and good thrust margins occur. The practical limit of this trend must be commensurate with heating and structural limitations on dynamic pressure, which correspond to a 71 820-Pa (1500-lbf/ft^2) acceleration trajectory for this research airplane concept.

CONCLUDING REMARKS

A preliminary study was conducted of scramjet engine-nozzle integration at hypersonic speeds, and the results of the analysis were applied to a highly integrated hypersonic research aircraft. As a result of the perturbation of major engine-airframe design parameters, several encouraging conclusions regarding scramjet-airframe integration have resulted. Foremost of these is that, with proper design, an efficient fixed-geometry engine-nozzle combination using the aircraft afterbody as an exhaust nozzle provides controlled and stable flight over a wide range of Mach numbers. The relative simplicity inherent in fixed-geometry nozzle concepts combined with fixed-geometry engine modules as compared with variable geometry systems should facilitate future scramjet propulsion-system development. Also significant from a total-vehicle-performance standpoint was the result that nozzle designs, which optimize at the high-speed end

of the flight envelope, also generally show superior performance at the low-speed end of the scramjet operating range. Thus, only a small penalty must be paid in nozzle performance at any Mach number for the fixed-geometry concept. For vehicle types similar to the one studied in this paper, only slight changes in basic aircraft stability are anticipated with the addition of engine modules to the vehicle undersurface and no major effect on power-on conditions was noted on longitudinal stability.

Owing to the preliminary nature of the study only major design trends were developed, and many important though second-order parameters were not considered. In particular, the sensitivity of nozzle design to three-dimensional flow variations was not assessed but should be included in more detailed future investigations. Future work must also be carried out in the area of vehicle dynamic behavior and control effectiveness during an engine shutdown situation. Although this study showed only moderate changes in elevon trim requirements between power-on and power-off engine conditions, the overall vehicle dynamic performance under such transient conditions is unknown.

Langley Research Center
National Aeronautics and Space Administration
Hampton, VA 23665
September 28, 1976

REFERENCES

1. Becker, John V.; and Kirkham, Frank S.: Hypersonic Transports. Vehicle Technology for Civil Aviation - The Seventies and Beyond, NASA SP-292, 1971, pp. 429-445.

2. Nagel, A. L.; and Becker, J. V.: Key Technology for Airbreathing Hypersonic Aircraft. AIAA Paper No. 73-58, Jan. 1973.

3. Becker, John V.: New Approaches to Hypersonic Aircraft. Paper presented at the Seventh Congress of the International Council of the Aeronautical Sciences (Rome, Italy), Sept. 1970.

4. Small, W. J.; Fetterman, D. E.; and Bonner, T. F., Jr.: Alternate Fuels for Transportation. Mech. Eng., vol. 96, no. 5, May 1974, pp. 18-24.

5. Gregory, Thomas J.; Williams, Louis J.; and Wilcox, Darrell E.: The Air-breathing Launch Vehicle for Earth Orbit Shuttle - Performance and Operation. AIAA Paper No. 70-270, Feb. 1970.

6. Johnston, P. J.; Cubbage, J. M.; and Weidner, J. P.: Studies of Engine-Airframe Integration on Hypersonic Aircraft. AIAA Paper No. 70-542, May 1970.

7. Cubbage, James M.; and Kirkham, Frank S.: Investigation of Engine-Exhaust-Airframe Interference on a Cruise Vehicle at Mach 6. NASA TN D-6060, 1971.

8. Kirkham, Frank S.; Cubbage, James M.; Vahl, Walter A.; and Small, William J.: Studies of Airframe-Propulsion-System Integration for Mach 6 Cruise Vehicles. NASA TN D-4128, 1967.

9. Anderson, Griffin Y.: An Examination of Injector/Combustor Design Effects on Scramjet Performance. NASA paper presented at the 2nd International Symposium on Air Breathing Engines (Sheffield, England), Mar. 25-29, 1974.

10. Edwards, C. L. W.: A Forebody Design Technique for Highly Integrated Bottom-Mounted Scramjets With Application to a Hypersonic Research Airplane. NASA TM X-71971, 1974.

11. Kirkham, F. S.; and Driver, C.: Energy Supply and Its Effect on Aircraft of the Future. Part II: Liquid-Hydrogen-Fueled Aircraft - Prospects and Design Issues. AIAA Paper No. 73-809, Aug. 1973.

12. Henry, John R.; and Beach, H. Lee: Hypersonic Airbreathing Propulsion Systems. Vehicle Technology for Civil Aviation - The Seventies and Beyond, NASA SP-292, 1971, pp. 157-172.

13. Henry, John R.; and Anderson, Griffin Y.: Design Considerations for the Airframe-Integrated Scramjet. NASA TM X-2895, 1973.

14. Gentry, Arvel E.; and Smyth, Douglas N.: Hypersonic Arbitrary-Body Aerodynamic Computer Program (Mark III Version). Rep. DAC 61552 (Air Force Contract Nos. F33615 67 C 1008 and F33615 67 C 1602), McDonnell Douglas Corp., Apr. 1968.
Vol. I - User's Manual. (Available from DDC as AD 851 811.)
Vol. II - Program Formulation and Listings. (Available from DDC as AD 851 812.)

15. Jackson, Robert J.; and Wang, Tennyson T.: Hypersonic Ramjet Experiment Project - Phase I. Computer Program Description Ramjet and Scramjet Cycle Performance. NASA CR-132454, 1974.

16. Dash, S.; and DelGuidice, P.: Analysis and Design of Three Dimensional Supersonic Nozzles. Volume I - Nozzle-Exhaust Flow Field Analysis by a Reference Plane Characteristics Technique. NASA CR-132350, 1972.

17. Kalben, P.: Analysis and Design of Three Dimensional Supersonic Nozzles. Volume II - Numerical Program for Analysis of Nozzle-Exhaust Flow Fields. NASA CR-132351, 1972.

TABLE 1.- ENGINE-INLET AND COMBUSTOR-EXIT CONDITIONS

$[\alpha = 2^{\circ}; \quad q_{\infty} = 71\,820 \text{ Pa}]$

M_{∞}	ϕ	p_1, Pa	T_1, K	V_1, m/sec	p_3, Pa	T_3, K	V_3, m/sec	Operational mode
4	1.0	10 366	244	1153	157 717	2343	1093	Ramjet
4	0	10 366	244	1153	17 888	338	1072	Ramjet
6	1.0	6 248	282	1753	101 027	2328	1621	Scramjet
6	0	6 248	282	1753	16 327	448	1655	Scramjet
10	1.5	3 840	353	2982	57 935	2222	2837	Scramjet
10	0	3 840	353	2982	14 172	772	2831	Scramjet

TABLE 2.- ISOLATED LIFT, DRAG, AND MOMENT COEFFICIENTS

Notes:

1. "A" point of application of forces.
2. Free-stream pressure has been subtracted from all surfaces prior to integrations.

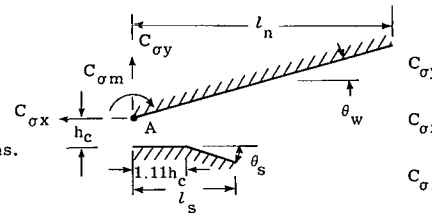

$C_{\sigma y} = \frac{\text{Lift}}{q_\infty A_c}$

$C_{\sigma x} = \frac{\text{Thrust}}{q_\infty A_c}$

$C_{\sigma m} = \frac{\text{Moment}}{q_\infty A_c l_n}$

θ_w	l_n/h_c	θ_s	l_s/h_c	ϕ	$C_{\sigma y}$	$C_{\sigma x}$	$C_{\sigma m}$	p_∞/q
				$M_\infty = 4$				
6.52	18.54	6.0	3.12	0	-0.536	-0.015	0.352	0.0893
6.52				1.0	1.966	.823	-.559	
12.02				0	-1.021	-.141	.547	
12.02				1.0	1.033	.994	-.272	
19.80		0		0	-1.467	-.358	.655	
		0		1.0	-.044	1.107	.149	
		6.0	1.50	0	-1.353	-.412	.737	
			1.50	1.0	.172	.802	.090	
			3.12	0	-1.442	-.397	.744	
			3.12	1.0	-.138	1.065	.009	
			4.50	0	-1.455	-.394	.747	
			4.50	1.0	-.325	1.113	.010	
		12.0	3.12	0	-1.347	-.418	.752	
		12.0	3.12	1.0	-.090	1.041	.085	
				$M_\infty = 6$				
6.52	18.54	6.0	3.12	0	0.157	0.076	0.061	0.0397
6.52				1	2.740	.777	-1.077	
12.02				0	-.338	.022	.108	
12.02				1	1.643	1.043	-.775	
19.80		0		0	-.934	-.129	.269	
		0		1	.186	1.183	-.631	
		6.0	1.50	0	-.645	-.169	.270	
			1.50	1	.795	.944	-.468	
			3.12	0	.771	-.128	.284	
			3.12	1	.371	1.203	-.524	
			4.50	0	-.871	-.114	.300	
			4.50	1	-.054	1.241	-.497	
		12.0	3.12	0	-.657	-.138	.275	
		12.0	3.12	1	.280	1.167	-.420	
				$M_\infty = 10$				
6.52	18.54	6.0	3.12	0	0.431	0.103	-0.244	0.0143
6.52				1.5	2.260	.575	-1.069	
12.02				0	-.062	-.075	.083	
12.02				1.5	1.217	.757	.838	
14.83	27.02		1.50		1.565	.706	-.605	
			3.12		.996	.864	-.862	
			4.50		.556	.928	-.687	
19.80	18.54	0	3.12	0	-.656	-.034	.109	
		0	3.12	1.5	-.090	.796	-.705	
		6.0	1.50	0	-.329	-.034	-.077	
			1.50	1.5	.703	.644	-.563	
			3.12	0	.443	-.019	.087	
			3.12	1.5	.102	.811	-.607	
			4.50	0	-.545	-.008	.108	
			4.50	1.5	-.351	.845	-.501	
		12.0	3.12	0	------	------	------	
		12.0	3.12	1.5	.208	.761	.475	
28.66	11.26	6.0	1.50		-.228	.462	-.395	
			3.12		-1.047	.548	-.219	
			4.50		-1.470	.592	-.074	

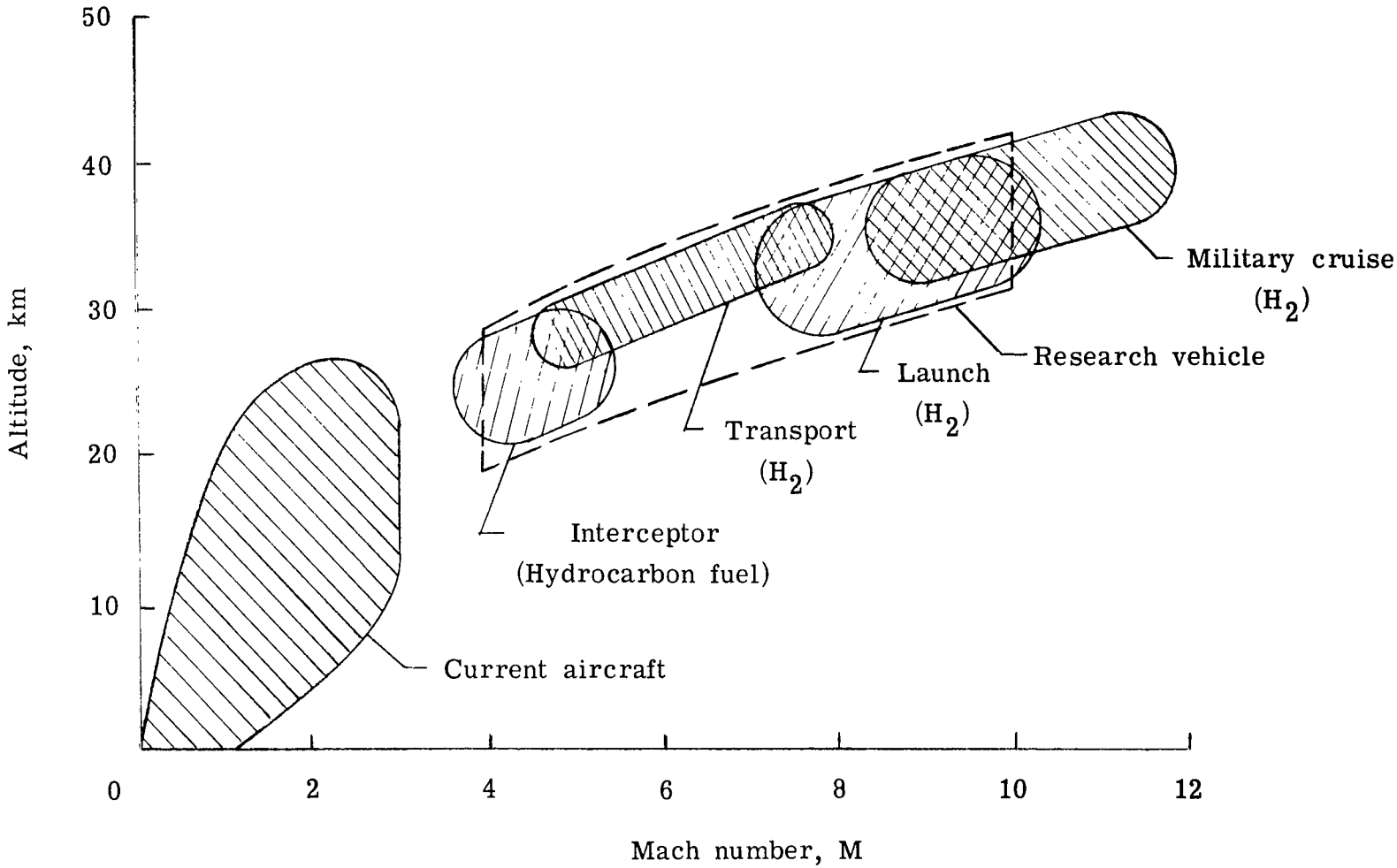

Figure 1.- Hypersonic flight envelope.

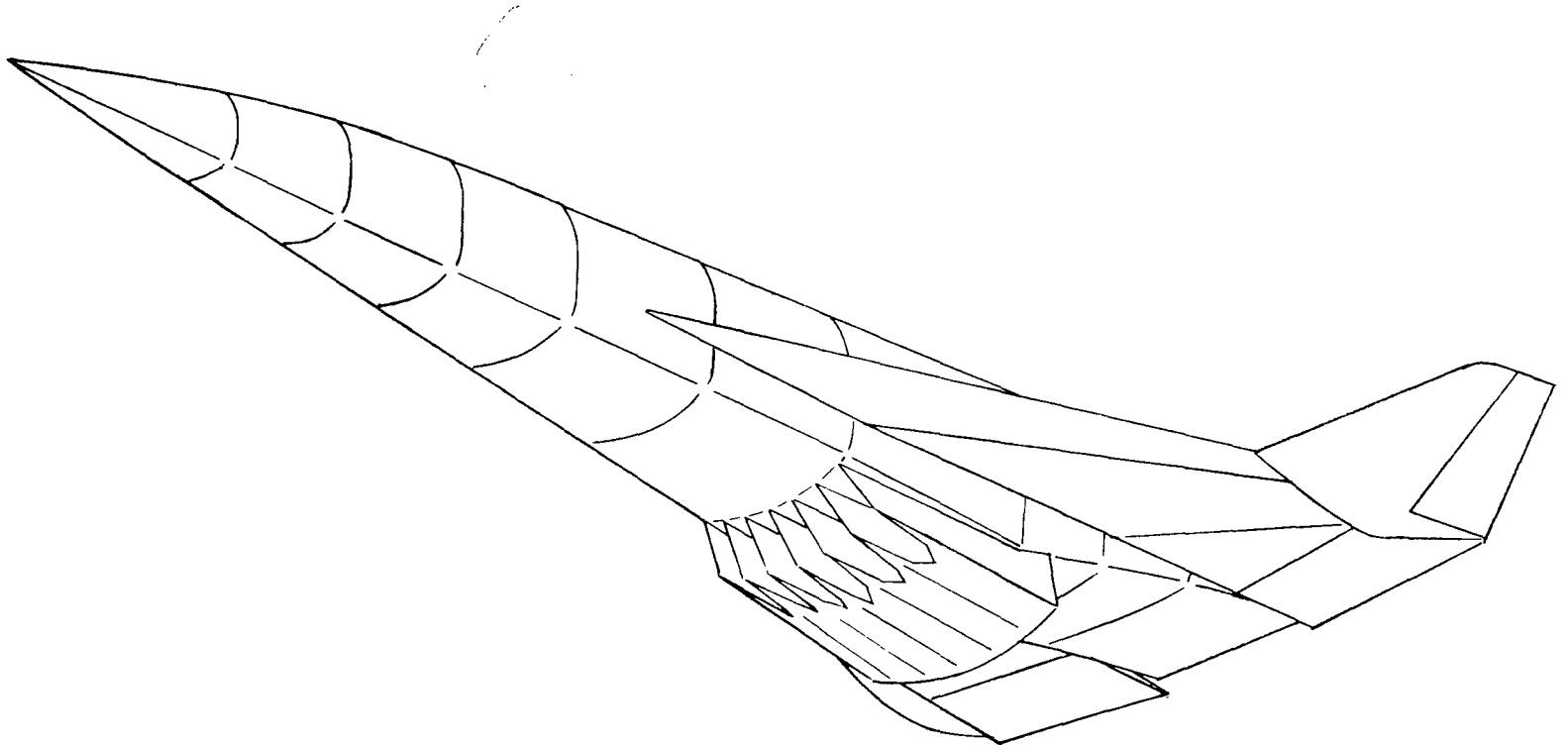

Figure 2.- Hydrogen-fueled research airplane.

Length, l_v = 24.38 m (80 ft)

Span = 10.67 m (35 ft)

Reference area = 99.89 m^2 (1075.2 ft^2)

Combustor-exit area/Inlet area = 0.602

Elevon area/Reference area = 0.115

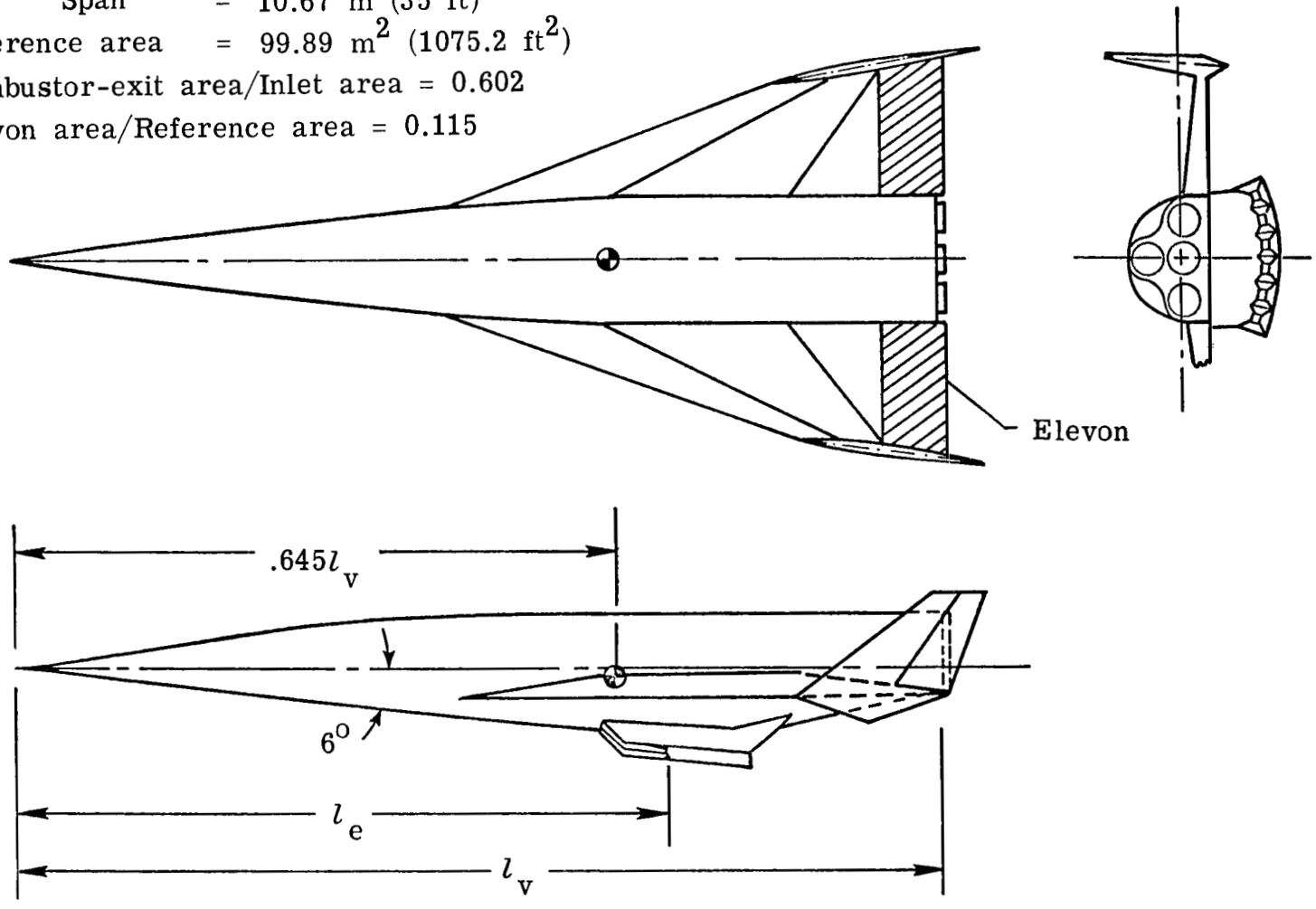

Figure 3.- Hydrogen-fueled research airplane concept.

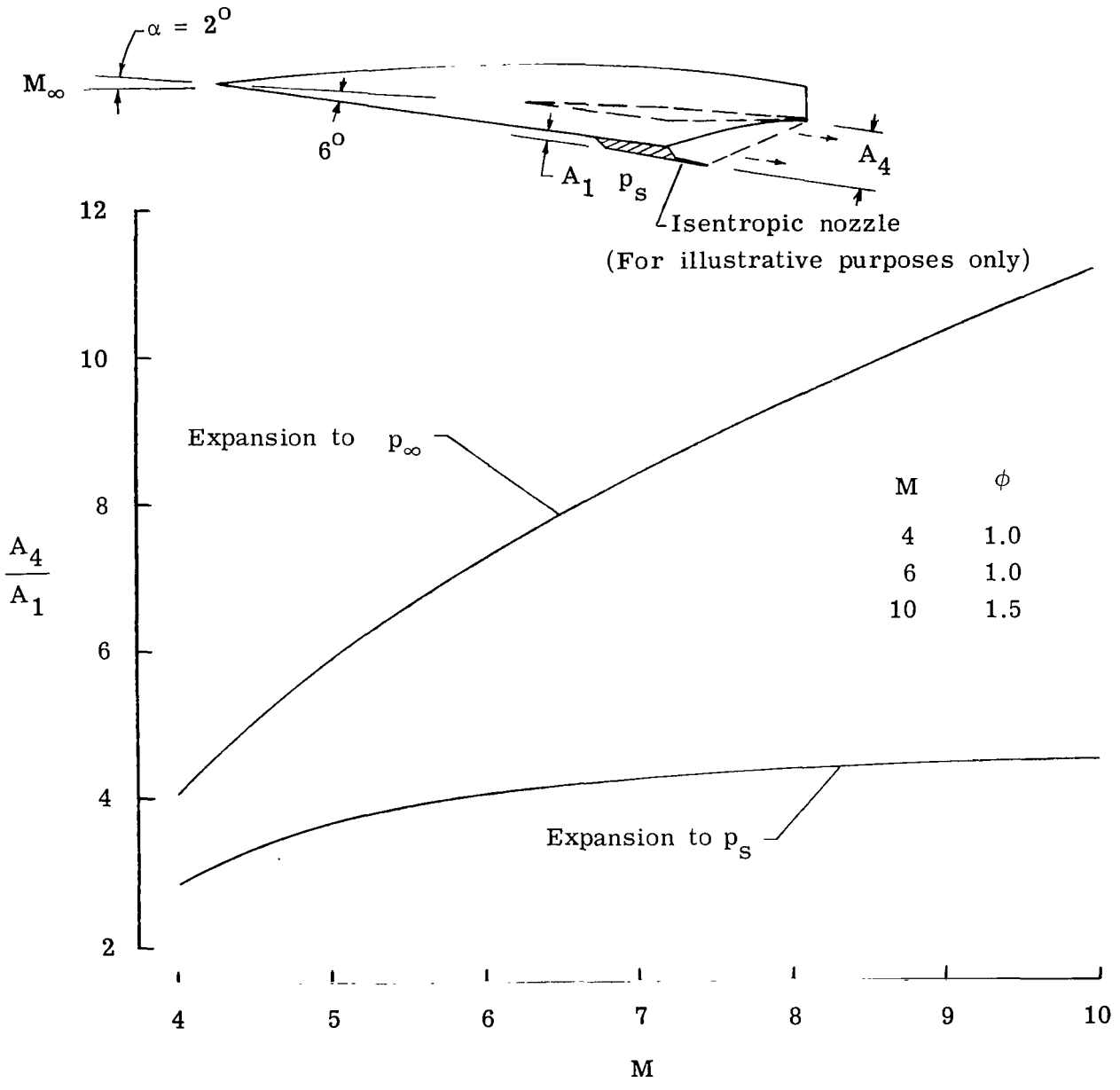

Figure 4.- Ideal nozzle-area-expansion hydrogen-air combustion-products chemical equilibrium. q_∞ = 71 820 Pa (1500 lbf/ft^2).

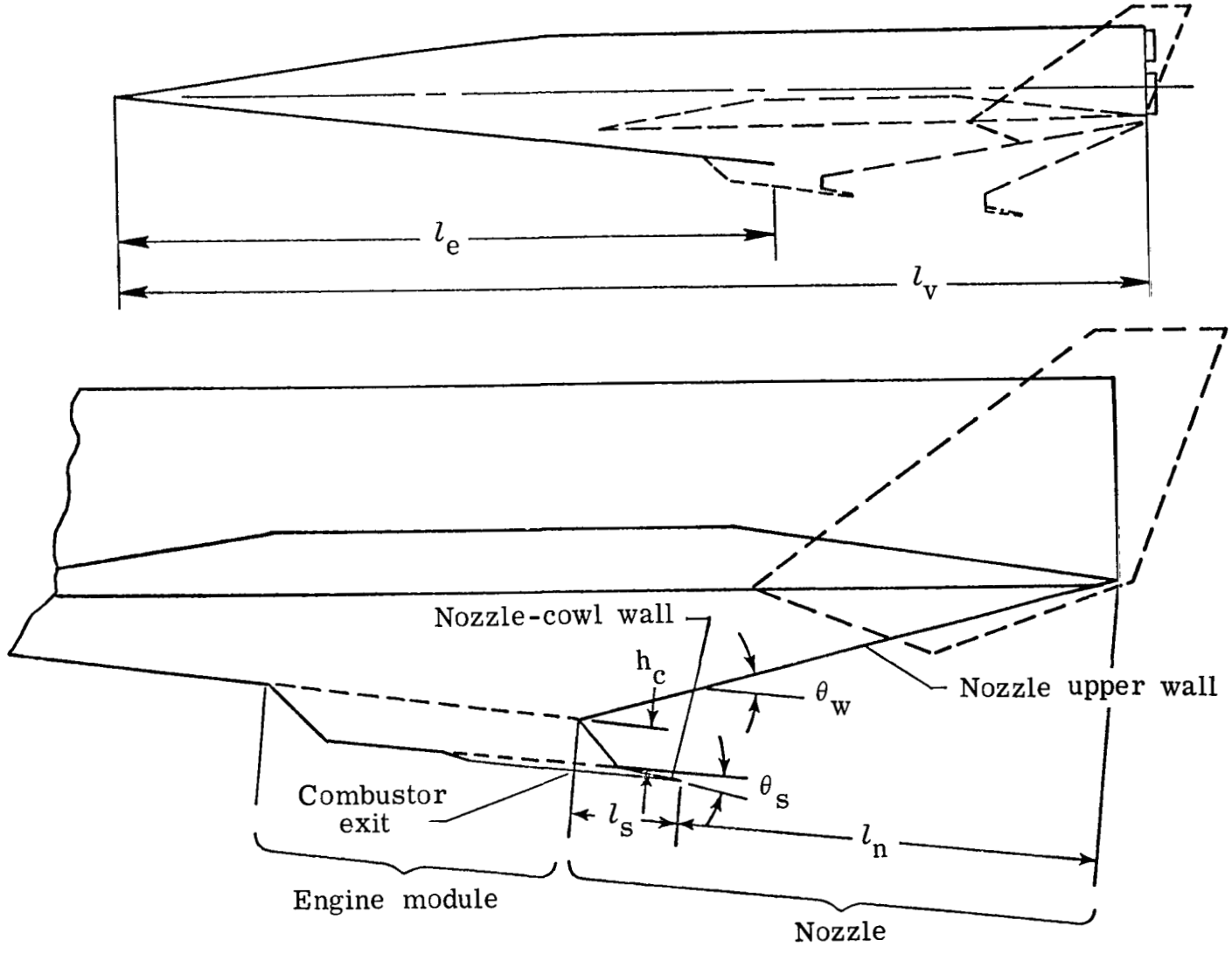

Figure 5.- Key nozzle optimization variables.

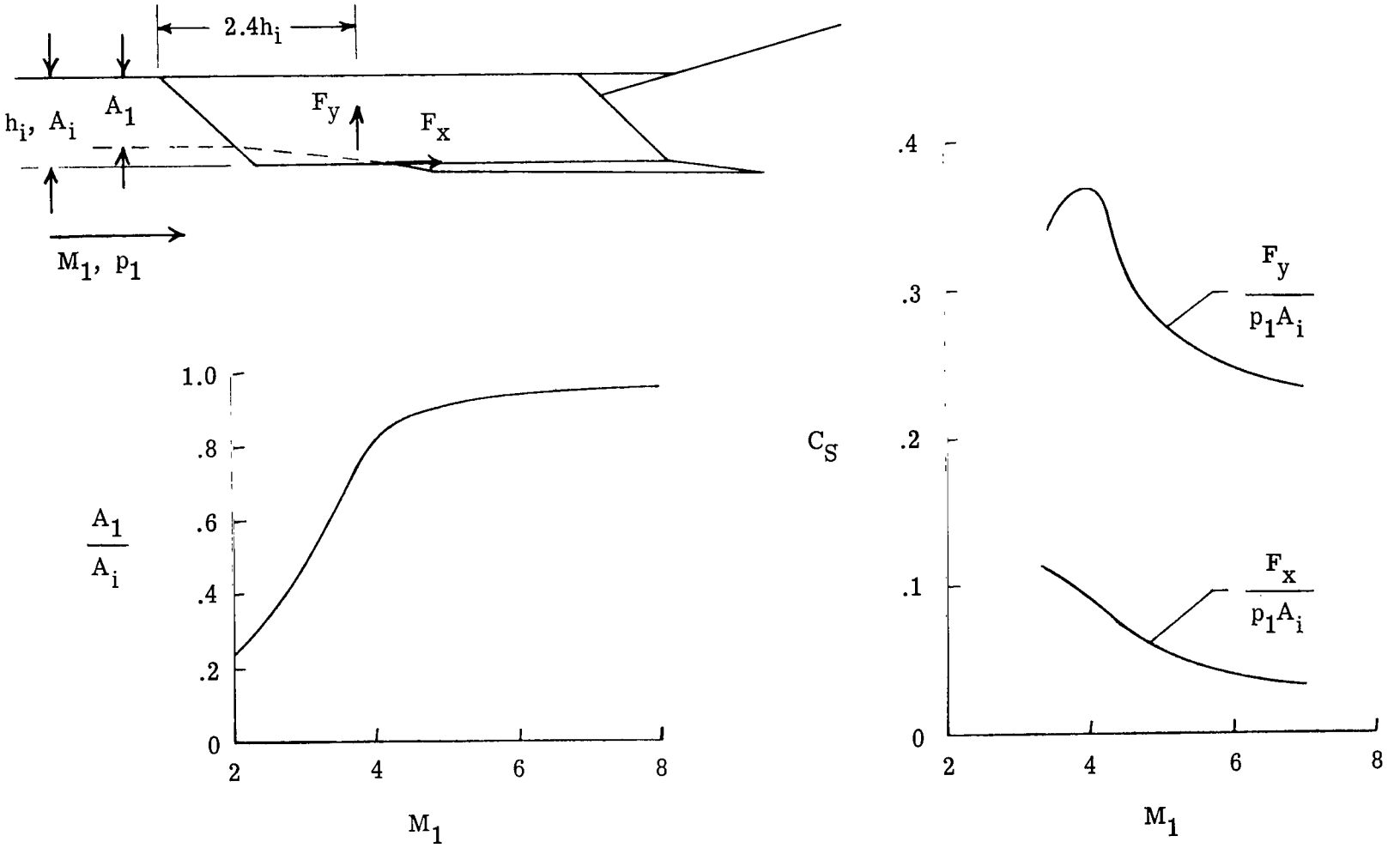

(a) Capture efficiency.

(b) Spillage forces.

Figure 6.- LRC scramjet-inlet capture-performance estimates.

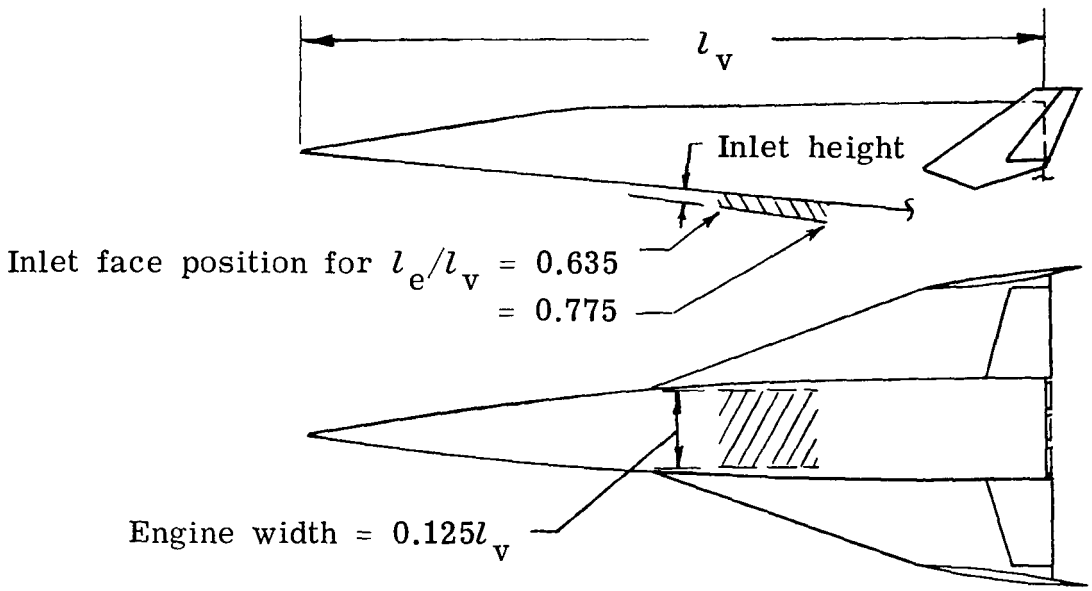

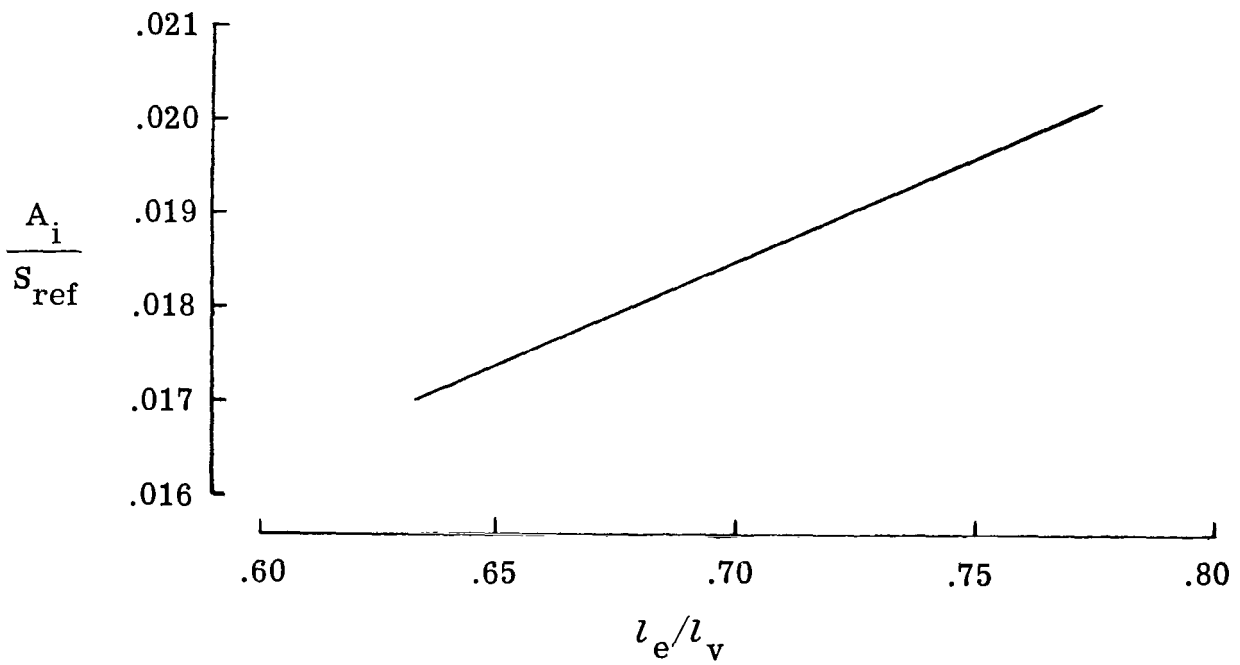

Figure 7.- Inlet-area variation along body length.

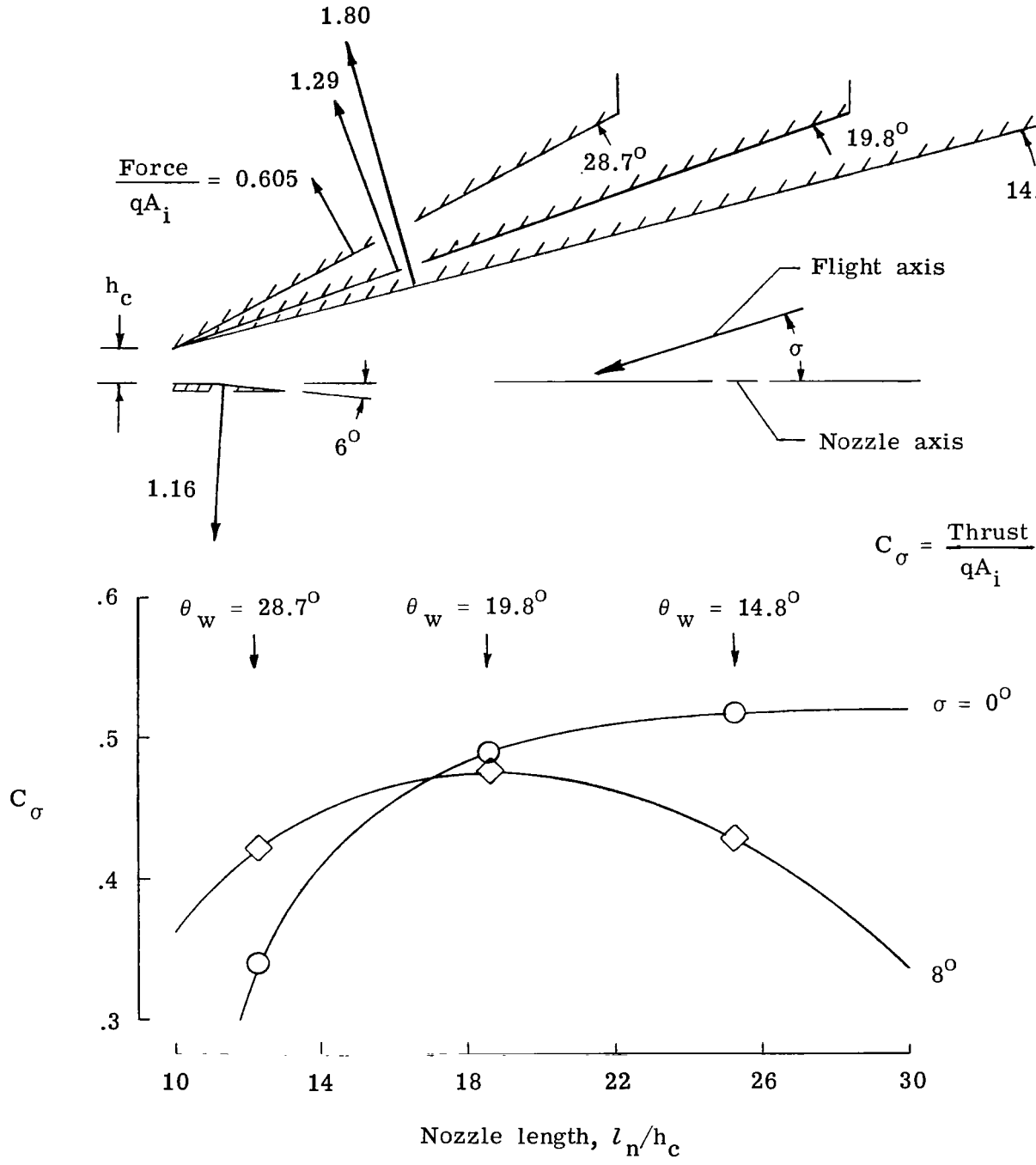

Figure 8.- Isolated-nozzle-force characteristics. M_∞ = 10; q = 71 820 Pa (1500 lbf/ft^2); ϕ = 1.5; l_s/h_c = 3.12.

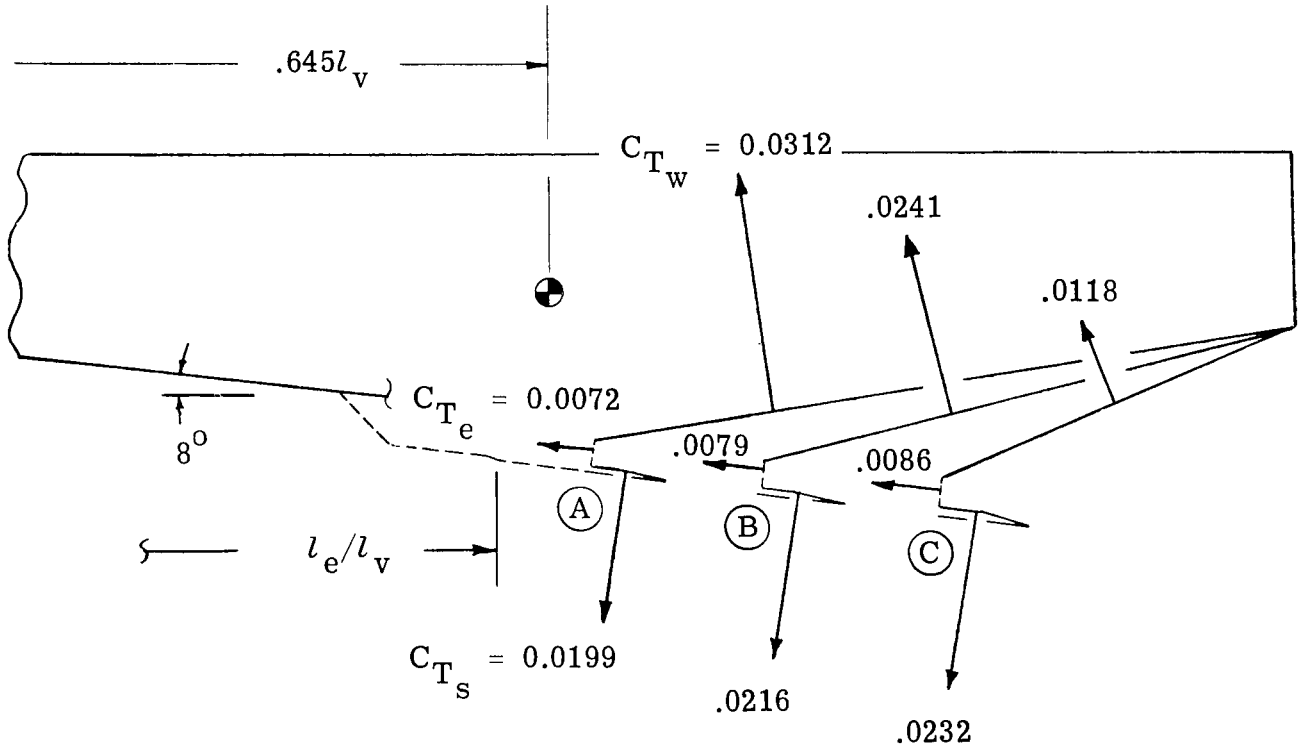

Nozzle	l_e/l_v	θ_w	θ_s
(A)	0.635	14.8	6
(B)	.694	19.8	6
(C)	.775	28.7	6

Figure 9.- Propulsion forces; axial scramjet location. M_∞ = 10; α = 2°; q = 71 820 Pa (1500 lbf/ft^2).

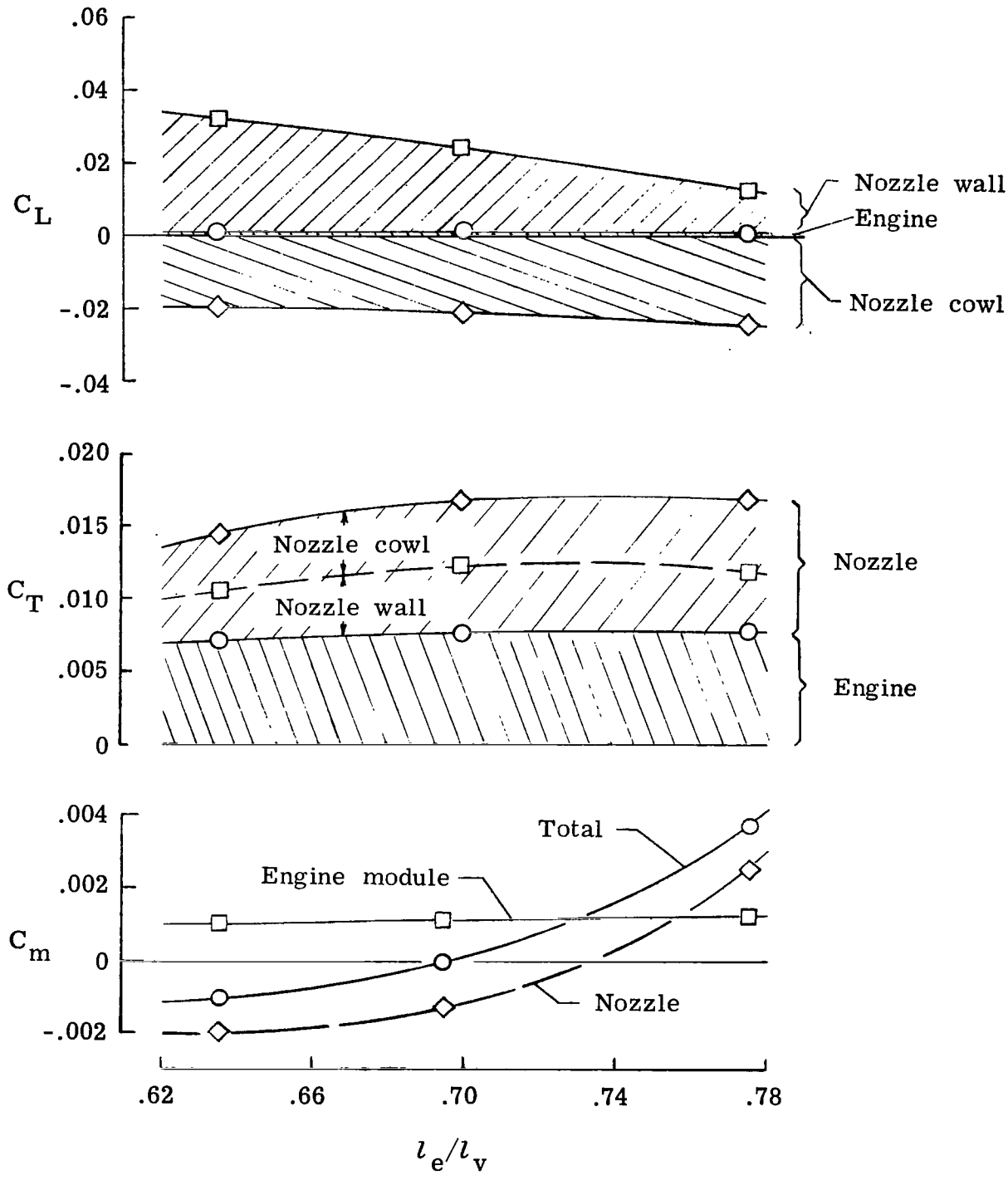

Figure 10.- Variation of scramjet location. $M_\infty = 10$; $\alpha = 2^\circ$; $q = 71\ 820$ Pa (1500 lbf/ft^2).

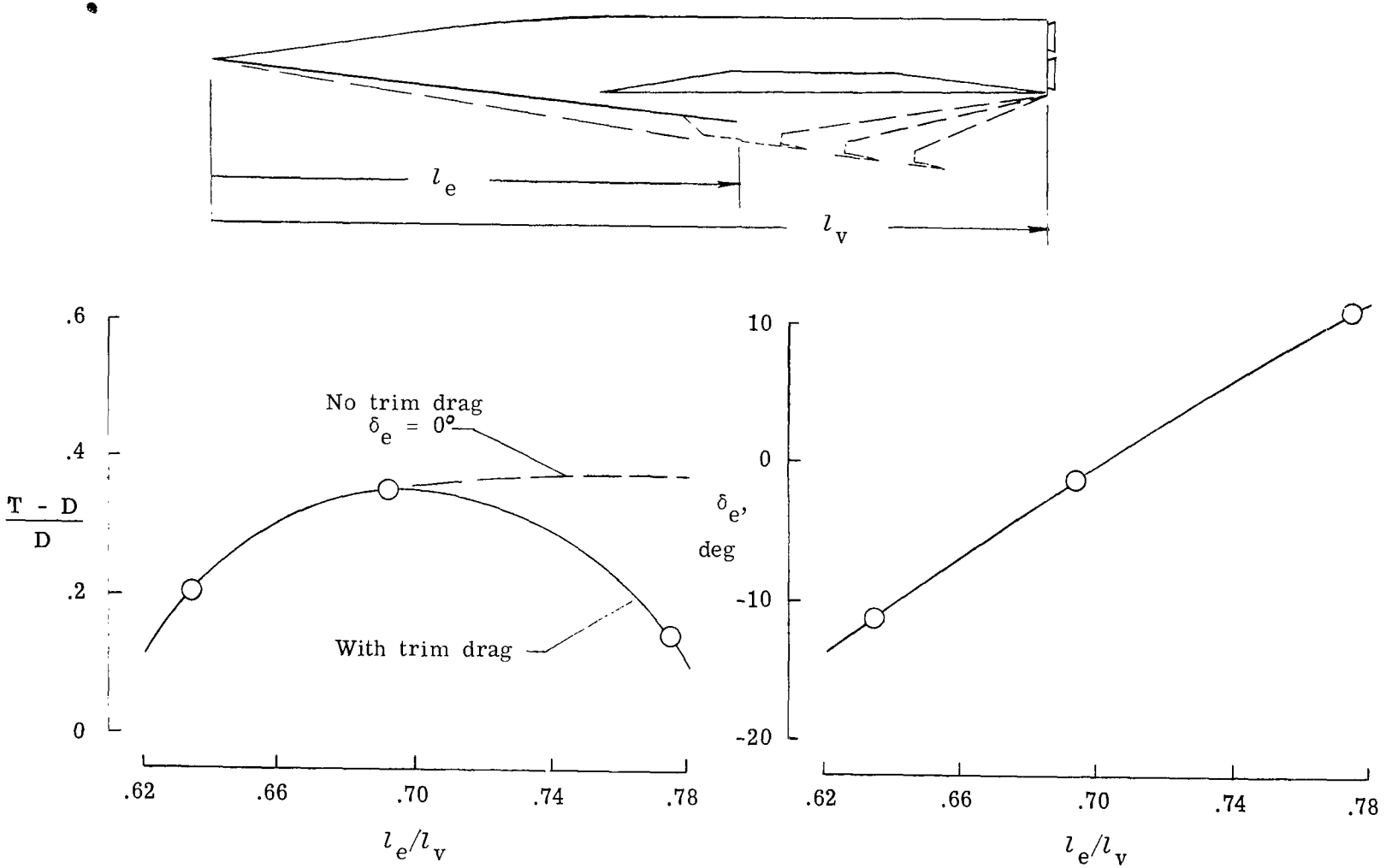

Figure 11.- Engine-axial-location (integrated) effects. M_∞ = 10; q = 71 820 Pa (1500 lbf/ft^2); $\alpha = 2^\circ$.

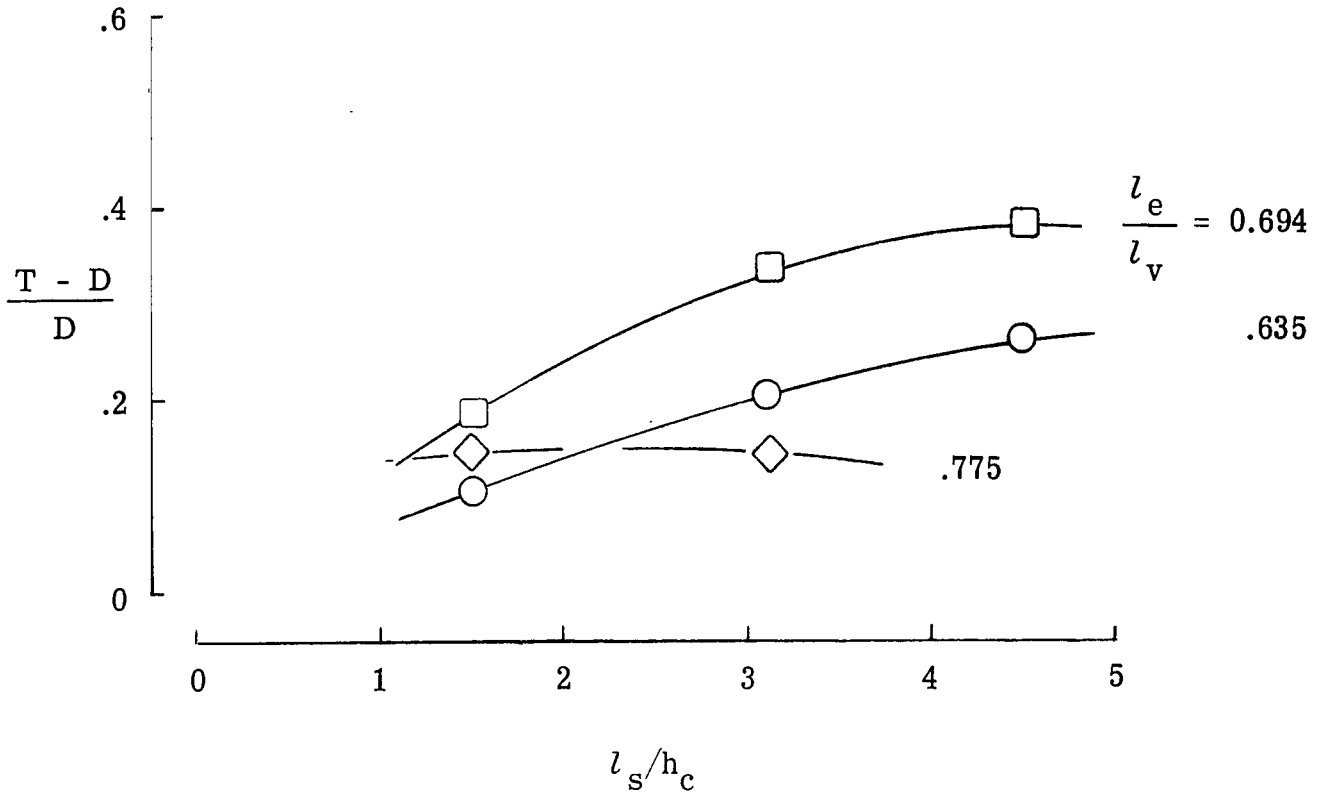

Figure 12.- Engine axial location (cowl-length effects). M_∞ = 10; ϕ = 1.5.

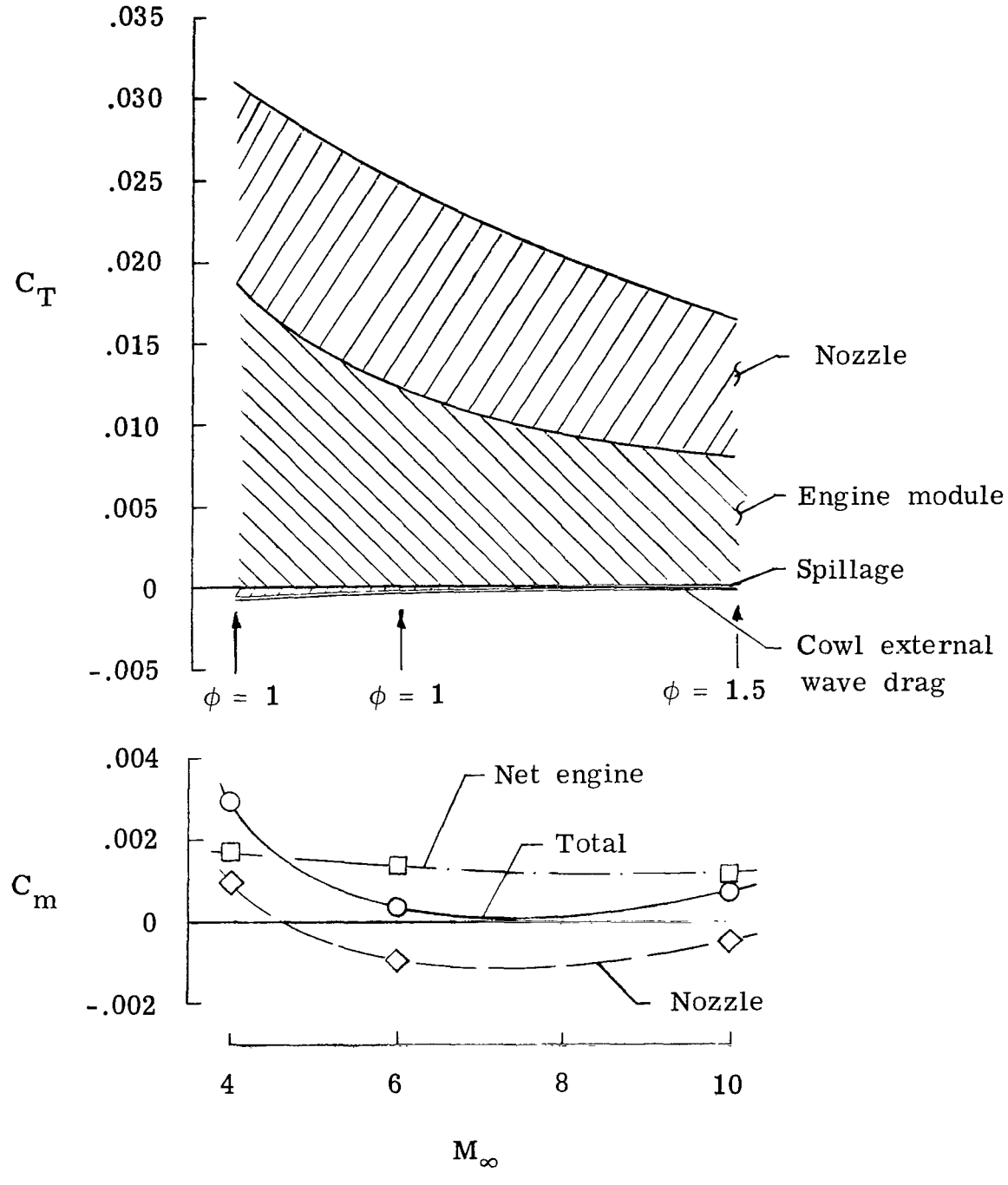

Figure 13.- Engine-nozzle thrust components. q = 71 820 Pa (1500 lbf/ft^2); α = 2.0°.

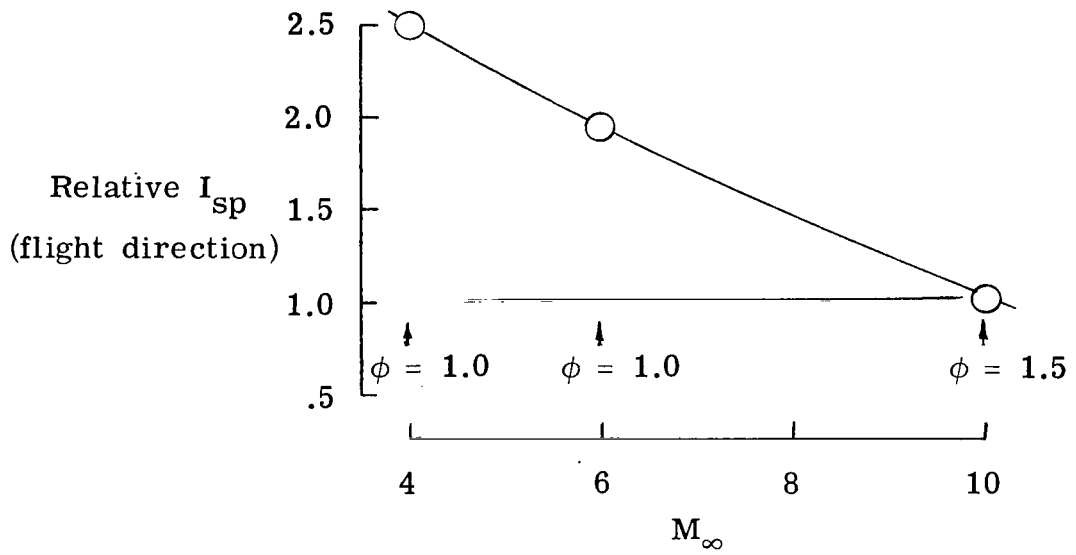

Figure 14.- Propulsion-system efficiency.
q = 71 820 Pa (1500 lbf/ft^2); α = 2.0°.

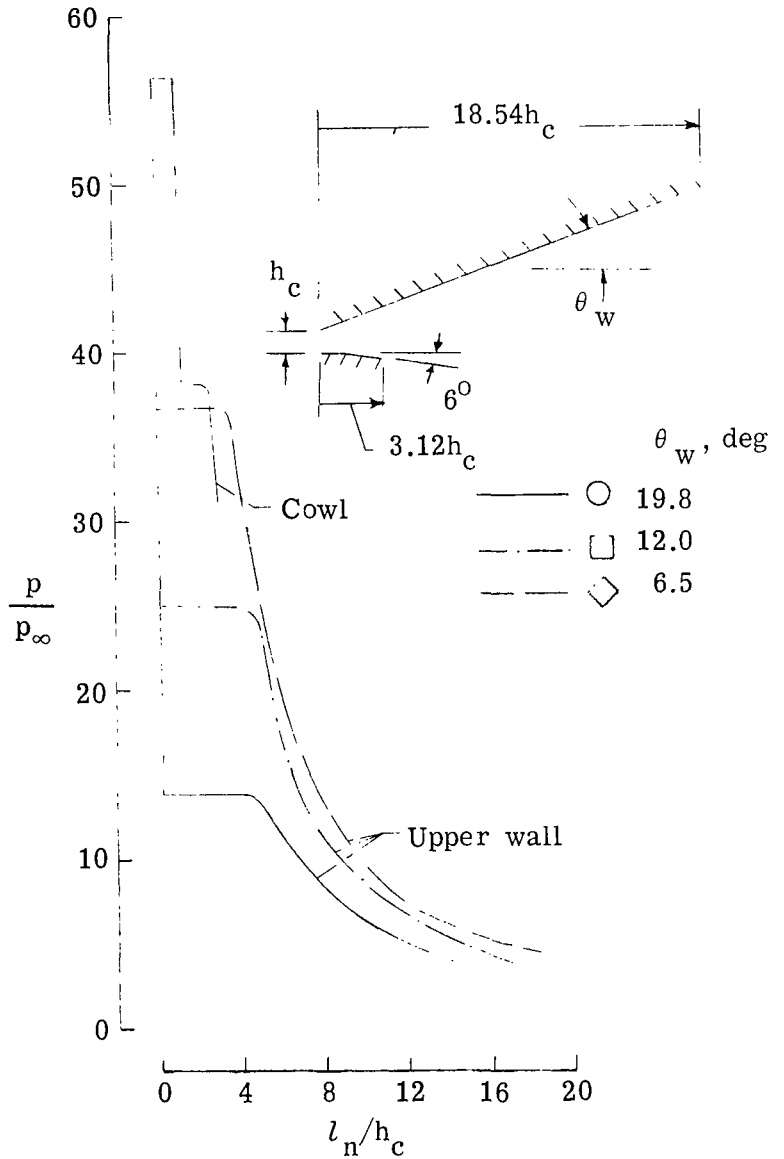

(a) Nozzle pressure distributions; M_∞ = 10.

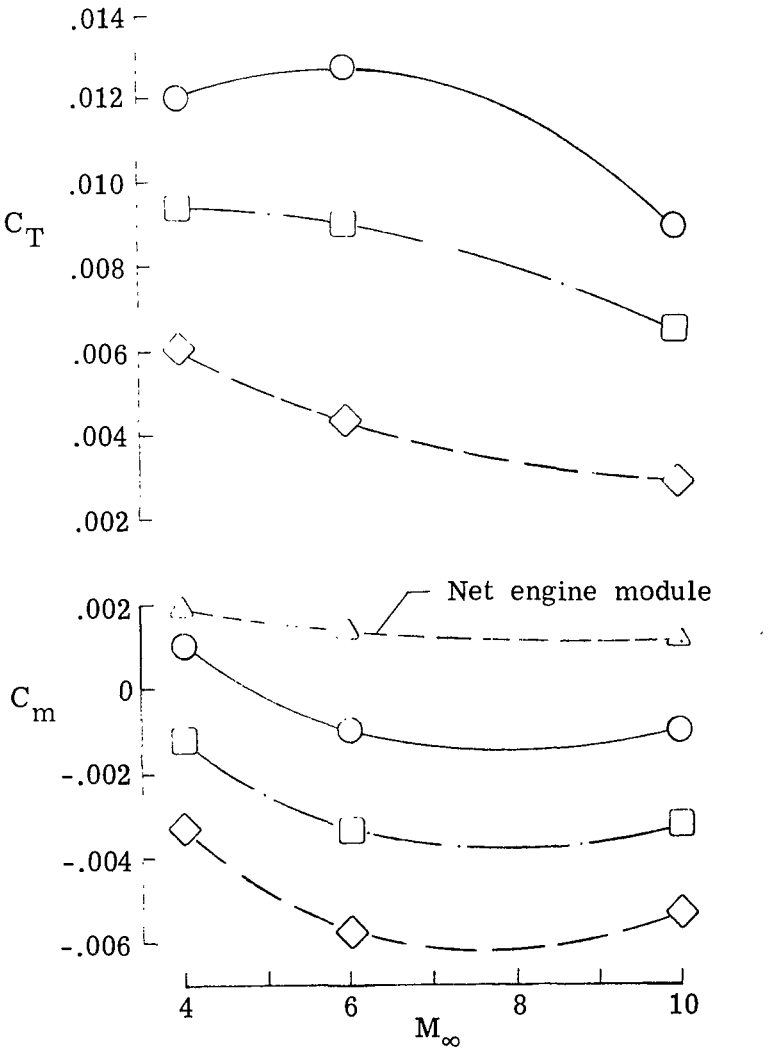

(b) Nozzle thrust and moments.

Figure 15.- Nozzle-wall angle variation. q = 71 820 Pa (1500 lbf/ft^2); $\alpha = 2^\circ$.

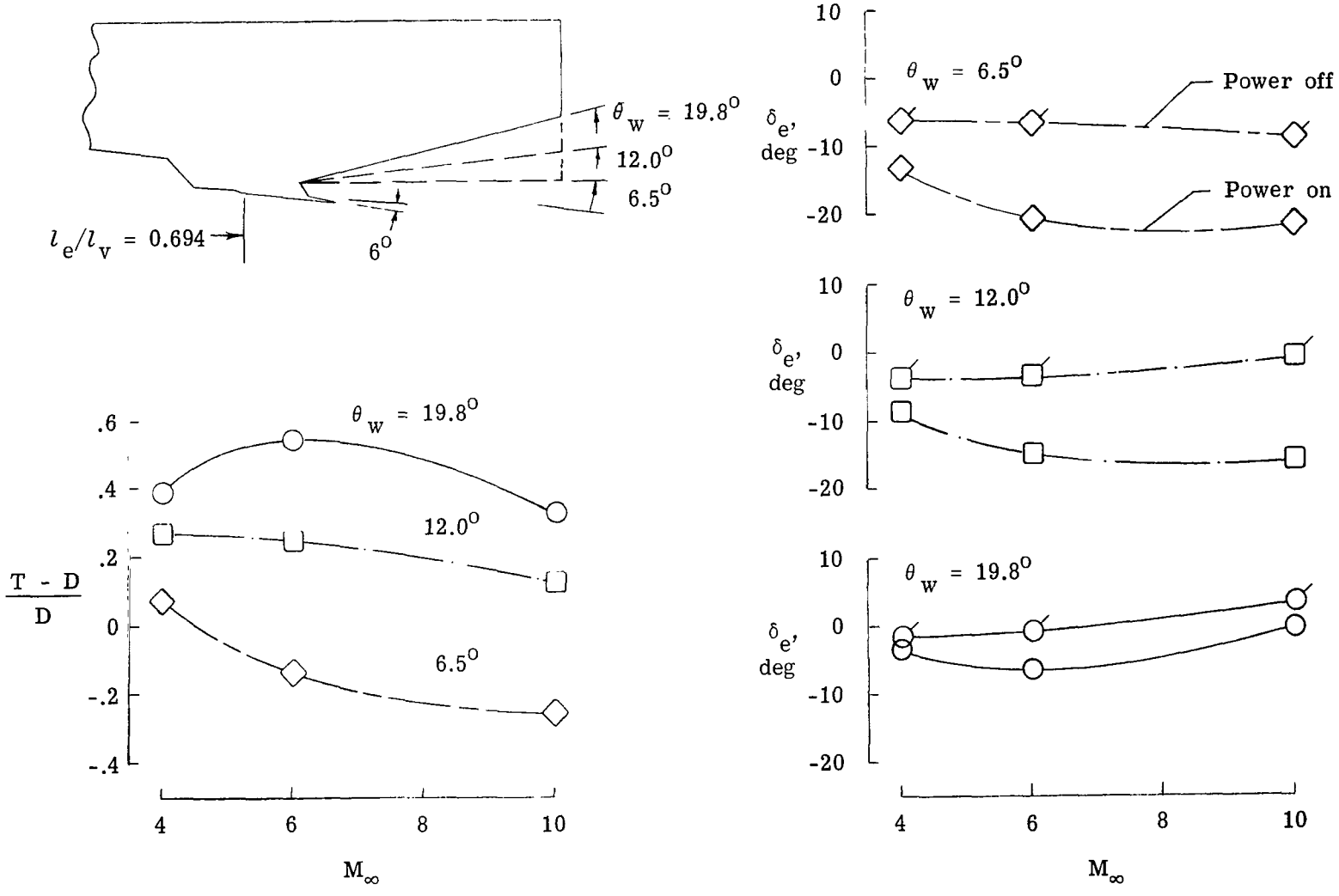

(a) Thrust margin.

(b) Elevon trim deflections.

Figure 16.- Nozzle-expansion effects. q = 71 820 Pa (1500 lbf/ft^2); α = 2°.

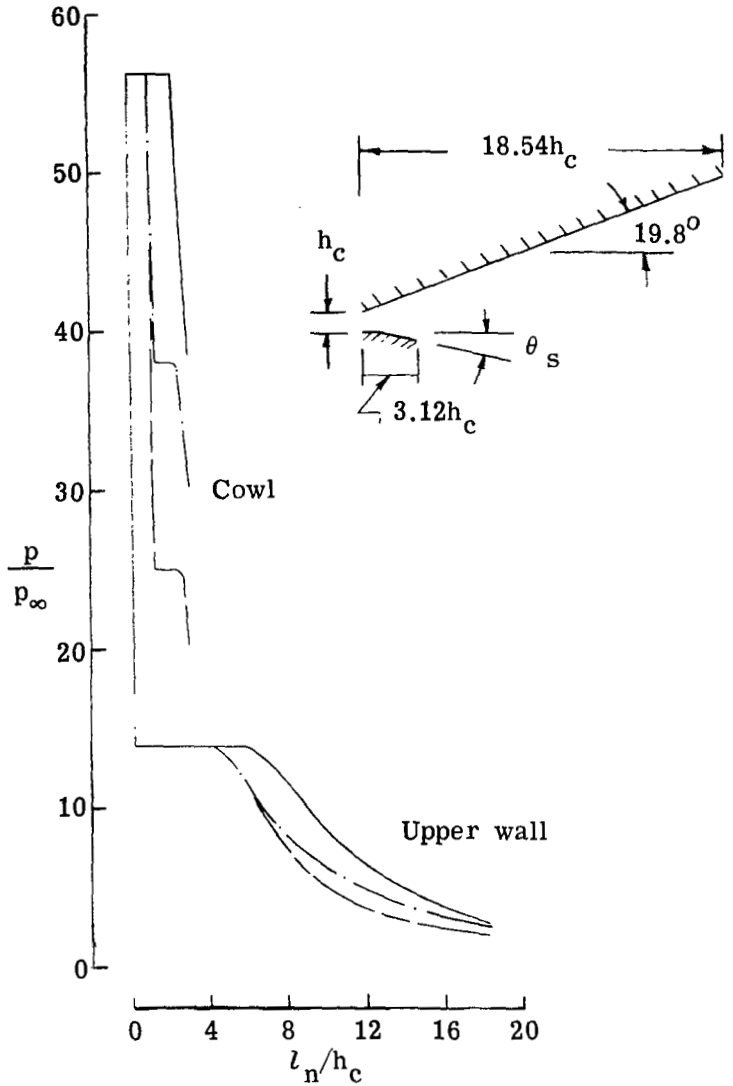

(a) Nozzle pressure distributions; $M_\infty = 10$.

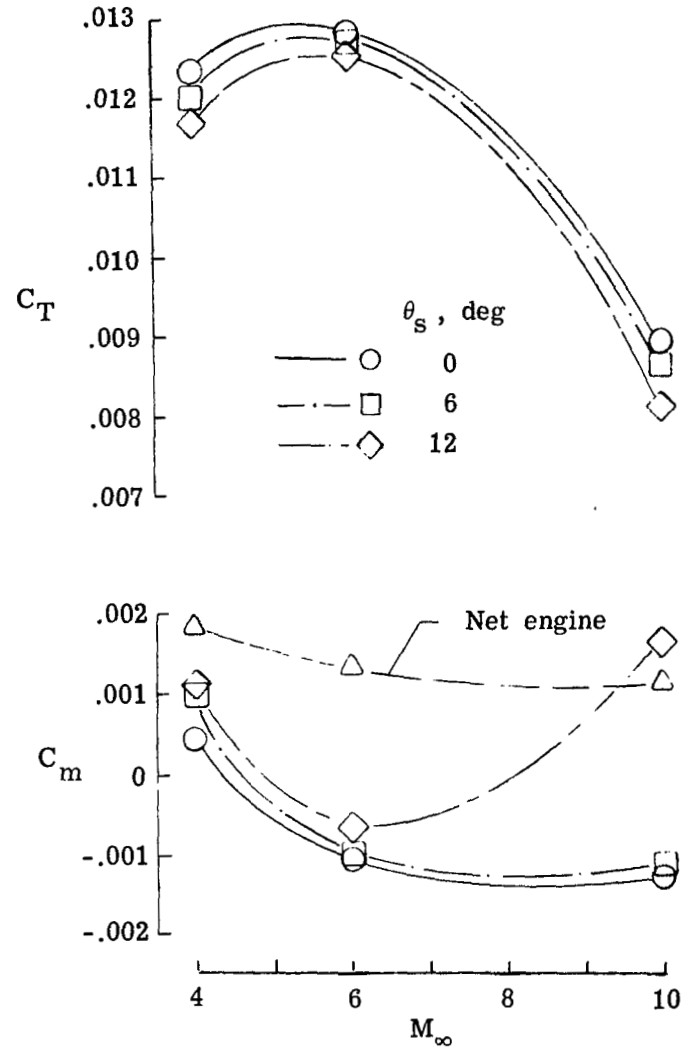

(b) Nozzle thrust and moments.

Figure 17.- Nozzle-cowl-angle variation. $q = 71\ 820$ Pa (1500 lbf/ft^2); $\alpha = 2^\circ$.

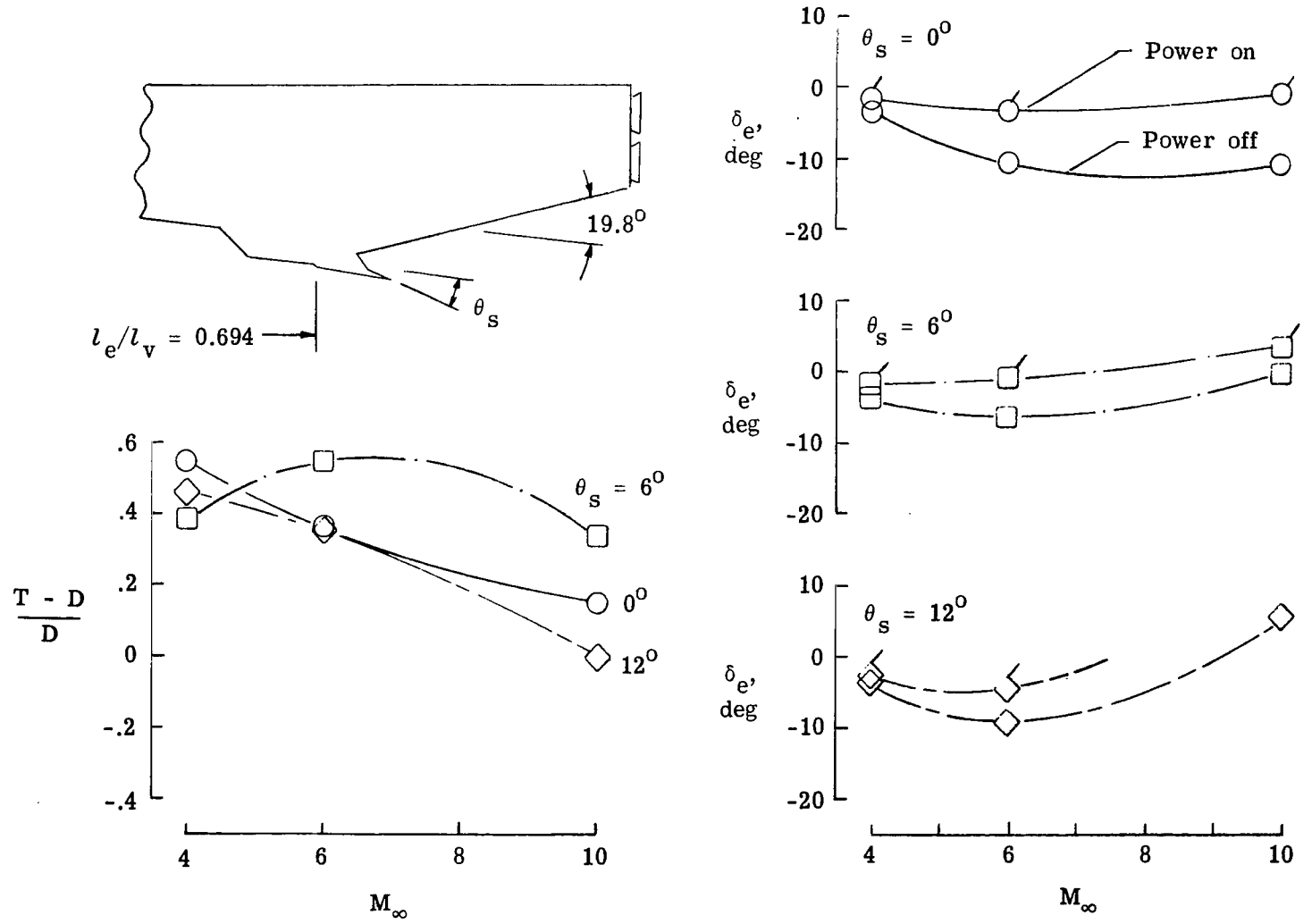

(a) Thrust margin.

(b) Elevon trim deflections.

Figure 18.- Nozzle-cowl-angle variation. q = 71 820 Pa (1500 lbf/ft^2).

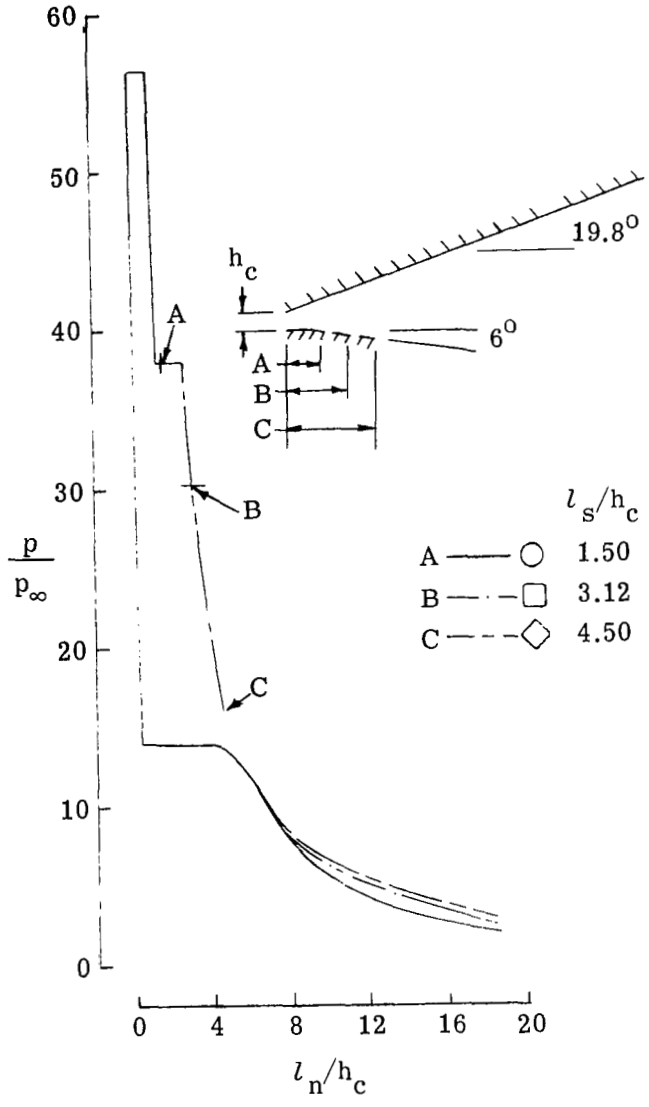

(a) Nozzle pressure distributions; $M_\infty = 10$.

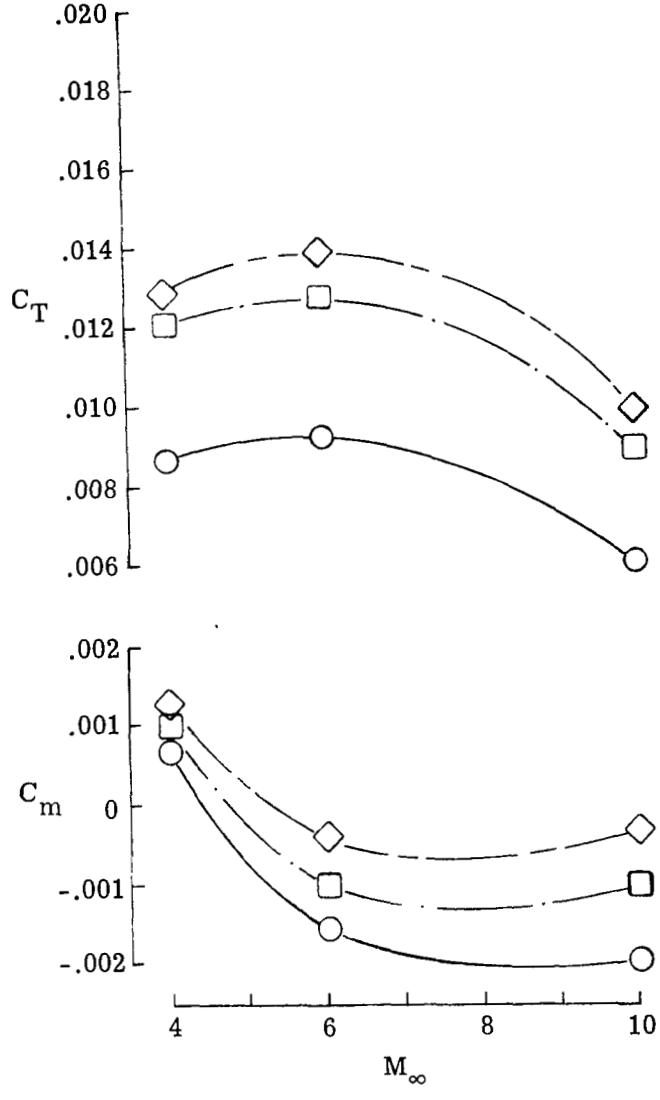

(b) Nozzle thrust and moments.

Figure 19.- Nozzle-cowl-length variation. q = 71 820 Pa (1500 lbf/ft^2); $\alpha = 2^\circ$.

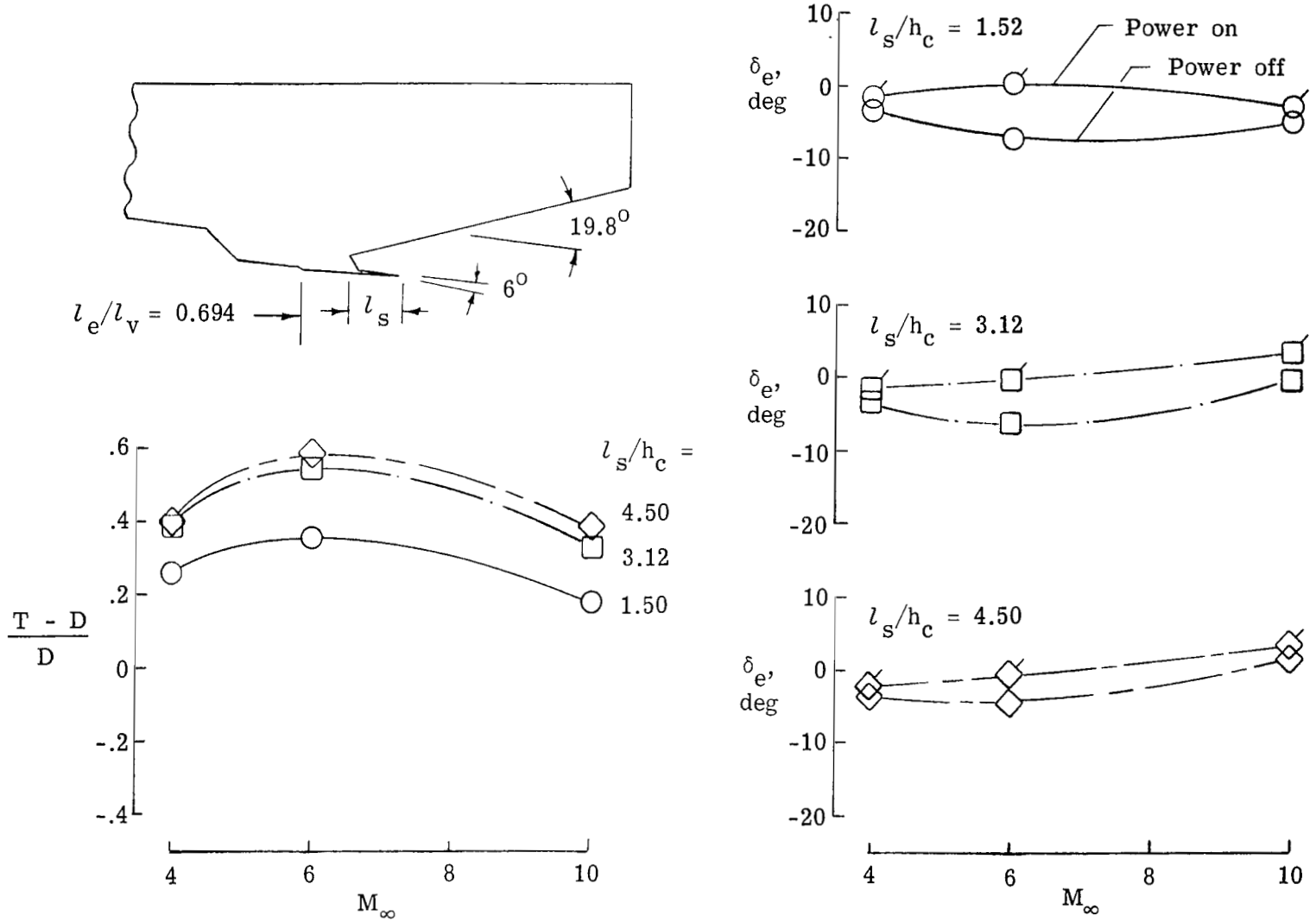

(a) Thrust margin.

(b) Elevon trim deflections.

Figure 20.- Nozzle-cowl-length variation. q = 71 820 Pa (1500 lbf/ft^2); $\alpha = 2^\circ$.

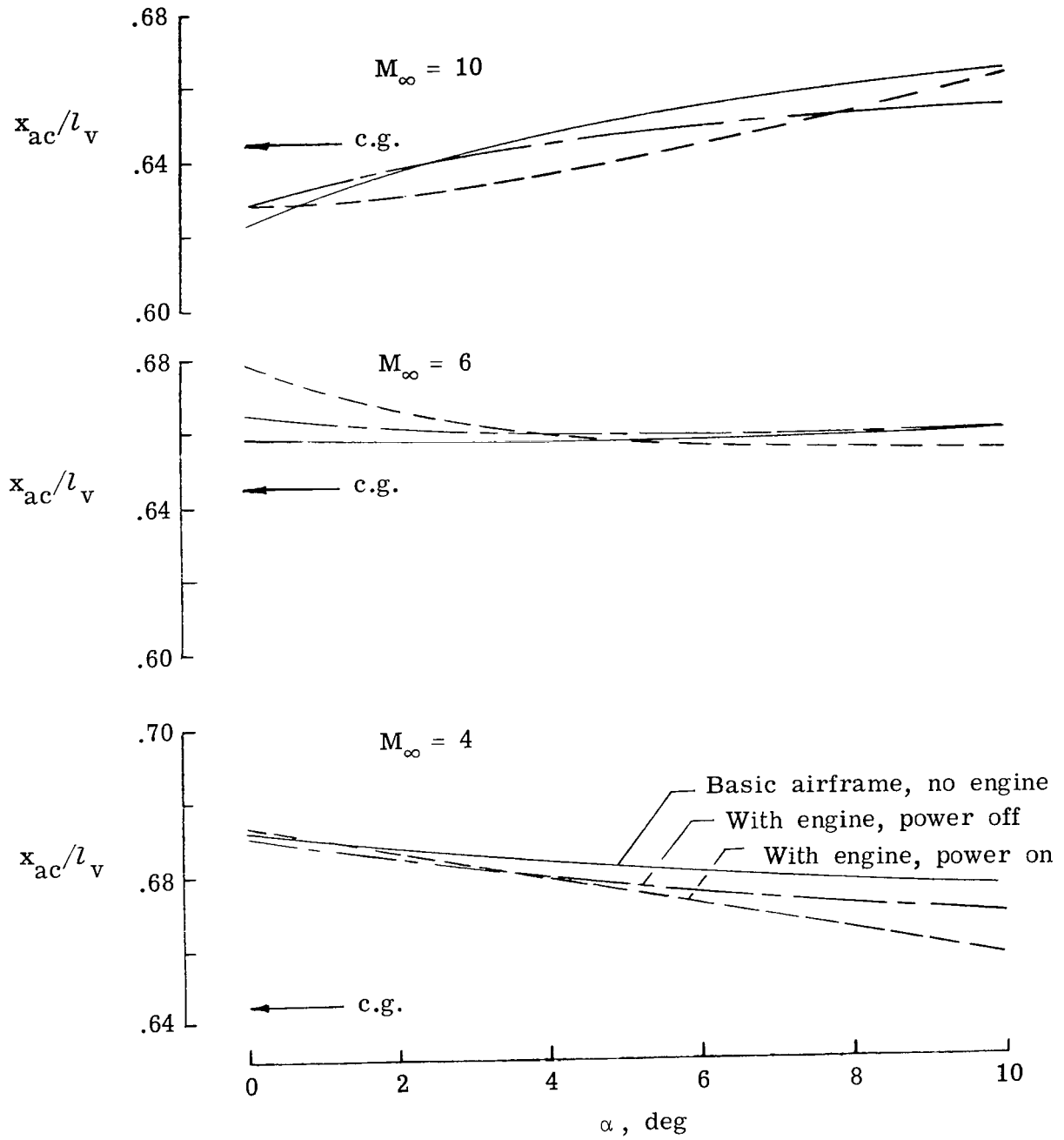

Figure 21.- Aerodynamic-center location. Vehicle c.g. = $0.645 l_v$; trimmed elevon setting.

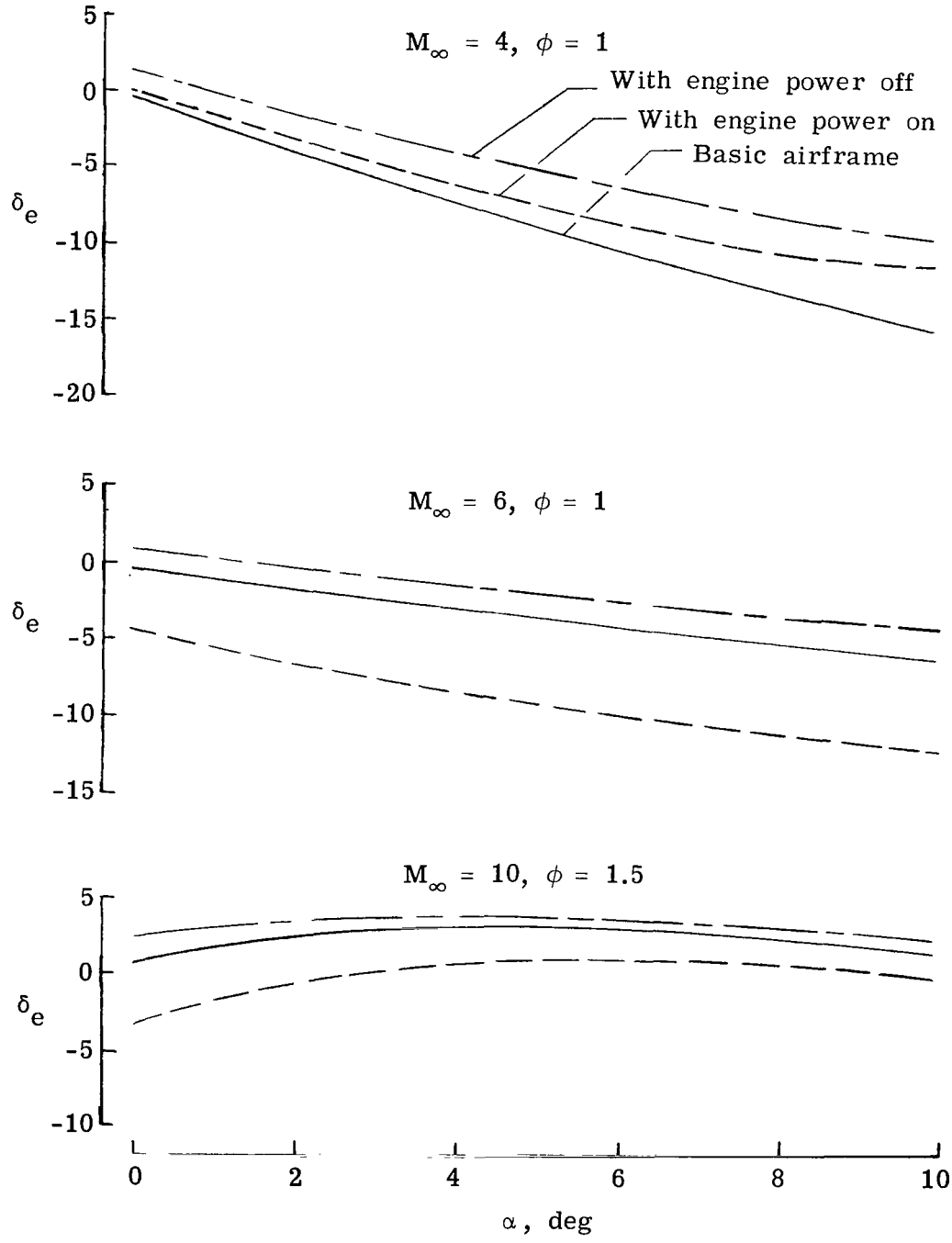

Figure 22.- Trim elevon deflections in pitch.
q = 71 820 Pa (1500 lbf/ft^2).

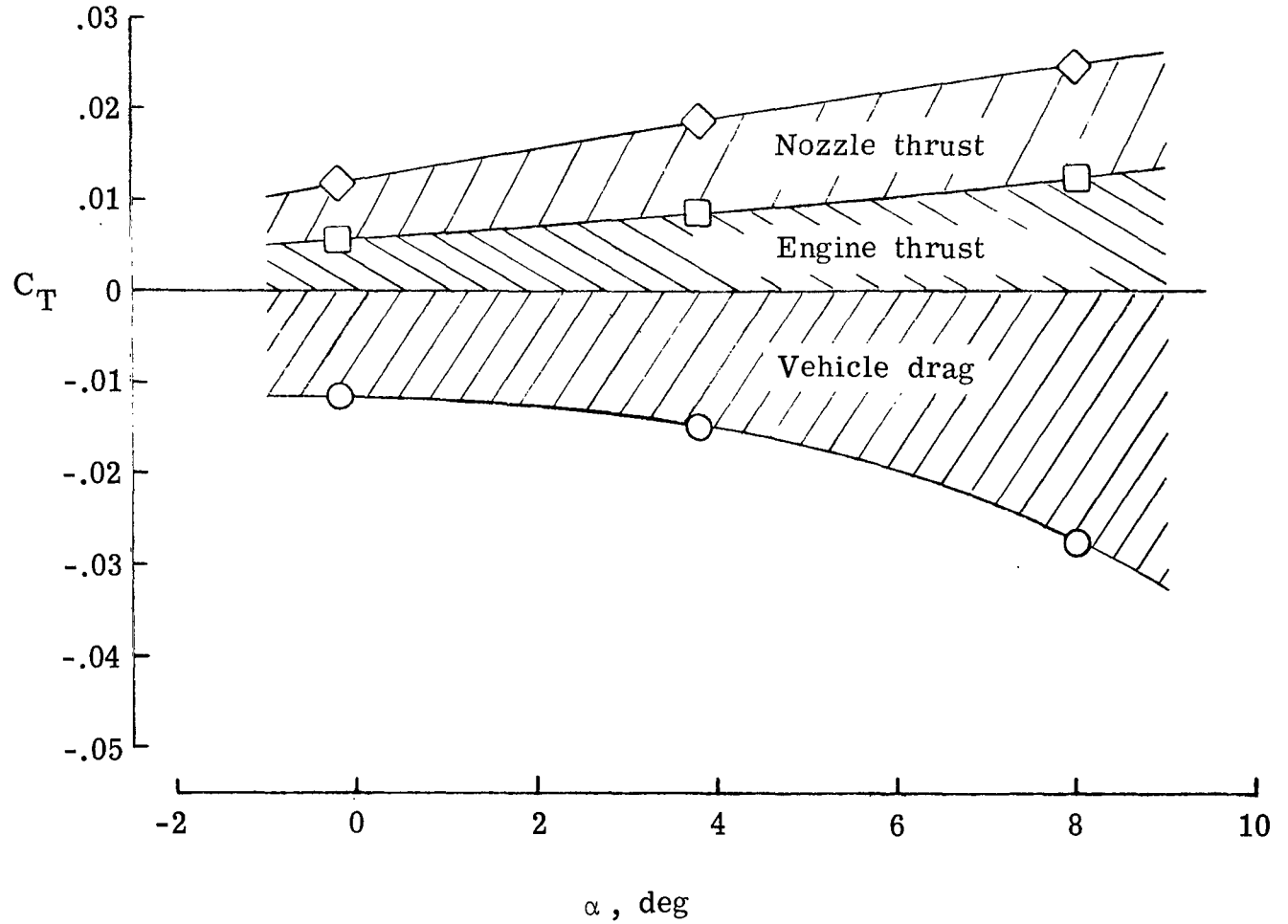

Figure 23.- Force components in flight direction. M_∞ = 10; q = 71 820 Pa (1500 lbf/ft^2).

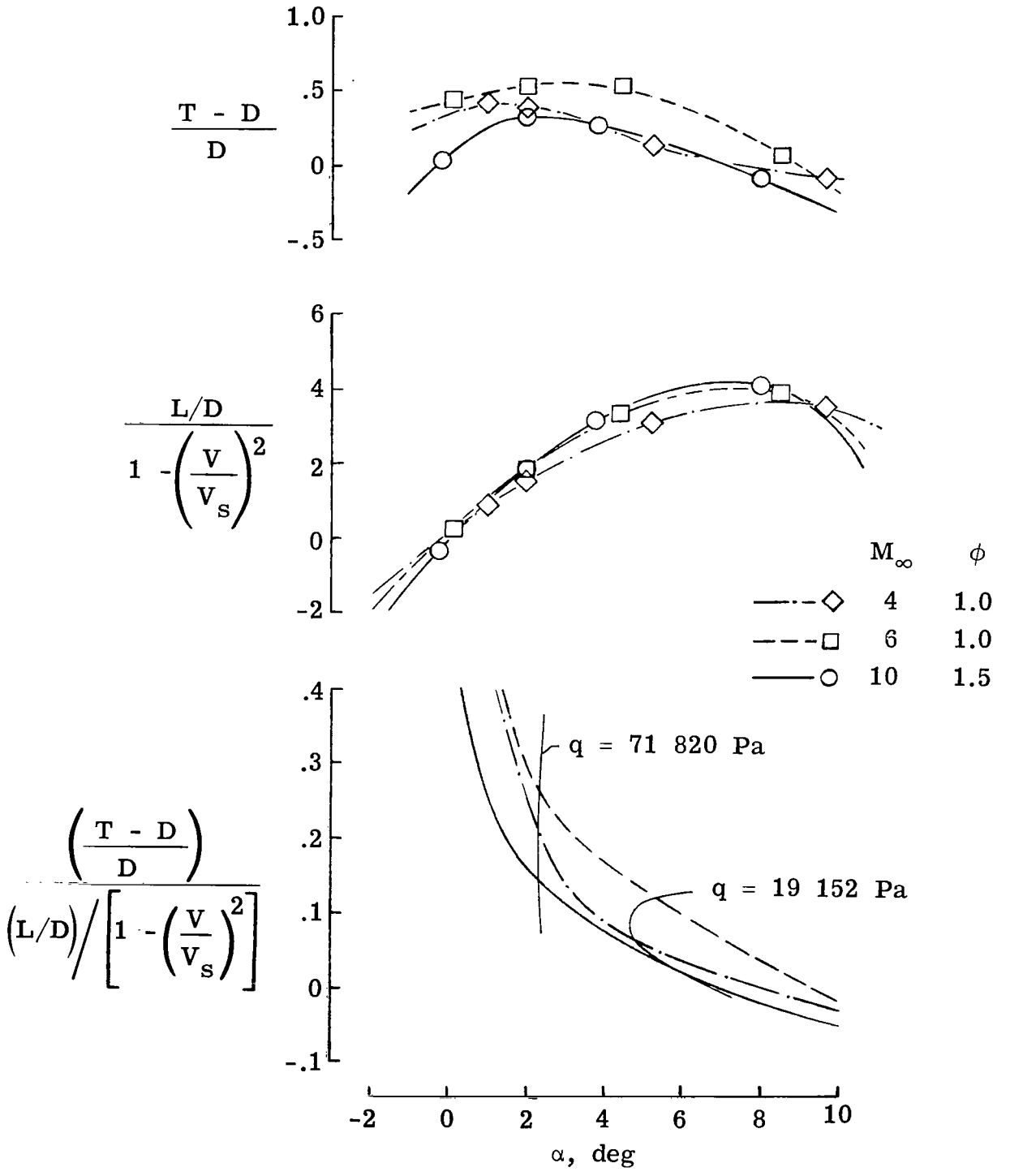

Figure 24.- Acceleration performance.

"The aeronautical and space activities of the United States shall be conducted so as to contribute . . . to the expansion of human knowledge of phenomena in the atmosphere and space. The Administration shall provide for the widest practicable and appropriate dissemination of information concerning its activities and the results thereof."

—NATIONAL AERONAUTICS AND SPACE ACT OF 1958

NASA SCIENTIFIC AND TECHNICAL PUBLICATIONS

TECHNICAL REPORTS: Scientific and technical information considered important, complete, and a lasting contribution to existing knowledge.

TECHNICAL NOTES: Information less broad in scope but nevertheless of importance as a contribution to existing knowledge.

TECHNICAL MEMORANDUMS: Information receiving limited distribution because of preliminary data, security classification, or other reasons. Also includes conference proceedings with either limited or unlimited distribution.

CONTRACTOR REPORTS: Scientific and technical information generated under a NASA contract or grant and considered an important contribution to existing knowledge.

TECHNICAL TRANSLATIONS: Information published in a foreign language considered to merit NASA distribution in English.

SPECIAL PUBLICATIONS: Information derived from or of value to NASA activities. Publications include final reports of major projects, monographs, data compilations, handbooks, sourcebooks, and special bibliographies.

TECHNOLOGY UTILIZATION PUBLICATIONS: Information on technology used by NASA that may be of particular interest in commercial and other non-aerospace applications. Publications include Tech Briefs, Technology Utilization Reports and Technology Surveys.

Details on the availability of these publications may be obtained from:

SCIENTIFIC AND TECHNICAL INFORMATION OFFICE

NATIONAL AERONAUTICS AND SPACE ADMINISTRATION

Washington, D.C. 20546